tion in the analysis of the correlation between the planes of the Dalitz pairs in π^0 decay.[7]

III. CONCLUSIONS

Under the conditions (a) and (b) enumerated above, the observation of a nonvanishing term proportional to $\sin 2\varphi$ in the distribution in the angle between the plane of the pair and the plane defined by its normal, $\mathbf{q}\times\mathbf{k}$, would indicate a nonvanishing interaction between a pair of K^+ mesons. Under condition (b) alone (which is perhaps the more likely of the two conditions to be fulfilled in reality), the absence of any correlation proportional to $\sin 2\varphi$ would imply that all meson-meson interactions were of negligible influence.[7a] This follows from the fact that time-reversal invariance requires $\mathrm{Re}\alpha^*\beta=0$ in the event that the low-energy $\bar{\Xi}^+-p$ elastic scattering is largely a diffraction effect (i.e., vanishing of the real part of the phase shifts) and that there are negligible meson-meson interactions in a system of pions and K mesons. This conclusion would not hold in the unlikely circumstance that only a single partial wave were produced in the two-K^+ system, for all values of $|\mathbf{q}|$, or in the circumstance that many partial waves conspired to give an accidental cancellation in the interference between the amplitudes α and β in Eq. (4), again for all values of $|\mathbf{q}|$.

Finally, we note that reaction (3) involves four positively charged particles, two with magnetic moments, and the possibility of the emission of a very energetic photon. All of these may contribute to an increased probability for this radiative process.

IV. ACKNOWLEDGMENT

The analysis in this note was stimulated by a remark made to the author by Professor Francis Low. Professor Low has applied a similar analysis to the process

$$K^+\rightarrow\pi^++\pi^0+\gamma, \qquad (15)$$

with subsequent materialization of the photon via creation of a pair. For this process, the presence or absence of a correlation proportional to $\sin 2\varphi$ could, in principle, clearly establish the existence or nonexistence, respectively, of a real pion-pion phase shift in the state of orbital angular momentum unity (but not in the S wave, owing to the absence of a zero-zero transition). I would like to thank Professor Low for his most helpful remarks.

[7] R. Plano *et al*, Phys. Rev. Letters 3, 525 (1959).

[7a] Under a similar condition, this statement could also be made with reference to a study of the reactions $\bar{p}+p\rightarrow 2\pi+\gamma$ and $\bar{p}+p\rightarrow K+\bar{K}+\gamma$.

PHYSICAL REVIEW VOLUME 120, NUMBER 1 OCTOBER 1, 1960

High-Energy Electron-Electron Scattering*

YUNG SU TSAI
Institute of Theoretical Physics, Department of Physics, Stanford University, Stanford, California
(Received May 10, 1960)

The radiative corrections to the electron-electron scattering to order α^3 are calculated for (1) the colliding beam experiment and (2) the experiment in which the target electron is at rest initially. The contributions from high-energy real photons are included. The two-photon exchange diagrams are found to give only negligible contributions to the cross sections after infrared cancellation. The effect due to the possible breakdown of quantum electrodynamics is discussed. A preliminary study on the electron-positron colliding beam experiment involving various interactions is made. The vacuum polarizations involving heavier particles than an electron pair in the closed loop are investigated.

I. INTRODUCTION

MANY experiments[1] have been suggested to test whether the electron has any finite size or if quantum electrodynamics (QED) is valid at small distances, say at 10^{-14} cm. Among them the interactions $e^-+e^-\rightarrow e^-+e^-$, $e^++e^-\rightarrow e^++e^-$, and $\gamma+e^-\rightarrow\gamma+e^-$ are pure quantum electrodynamical[2] or, in other words, they do not involve the structures of other particles whose effects are often difficult to distinguish from the effect due to the breakdown of QED at small distances. In this paper we are primarily concerned with the evaluation of cross sections for two specific experiments on electron-electron scattering by using the standard technique of QED to order α^3. Any significant deviation of the observed cross sections from the present calculation must be attributed to the breakdown of QED at small distances. The effect due to possible breakdown of QED at small distances is discussed in Sec. IV. The two experiments which we will proceed to discuss are as follows:

Experiment I. Electron-electron colliding beam experiment with two intersecting 500-Mev electron beams. The detectors for the scattered electrons are

* Supported in part by the U. S. Air Force through the Air Force Office of Scientific Research.

[1] S. D. Drell, Ann. Phys. 4, 75 (1958).

[2] Vacuum polarizations due to heavier particles than electrons are discussed in the Appendix. Their contributions to the cross sections are found to be negligible.

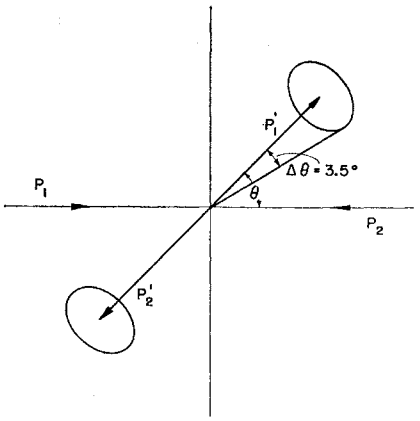

FIG. 1. Geometry for the electron-electron colliding beam experiment.

Čerenkov counters facing each other with equal circular apertures subtending the same solid angle and arranged for coincidence (see Fig. 1). Angular distributions (but not the absolute cross sections) from 35 to 90 degrees are taken.

Experiment II. Electron-electron scattering with the target electron at rest and the incident electron having energy $\bar{E}_1=500$ Mev (we use a bar to denote the quantities in the laboratory system for Exp. II). One of the outgoing electrons is undetected and the other electron is selected by a rectangular entrance slit and then entered into a spectrometer which selects the energies (see Fig. 6).

The first experiment is in progress at Stanford and is conducted by O'Neill, Barber, Gittelman, Panofsky, and Richter. It is designed to test the validity of QED at small distances down to $\approx 0.5\times 10^{-14}$ cm. The second experiment is also being carried out at Stanford, by Edgar B. Dally. The effect due to the breakdown of QED (if any) should not be observed in Exp. II due to the smallness of momentum transfer involved in the experiment. This calculation was originally started in order to calculate the cross section for Exp. I. However it was realized that the previous calculations on electron-electron scattering made by Redhead[3] and Polovin[4] do not apply to Exp. II; thus the calculation on Exp. II was included in this paper.

Redhead and Polovin calculated the radiative corrections to $e-e$ scattering with the target electron at rest in the laboratory system with the assumption that the maximum energy of the photon $\bar{K}_{\max}$ (we use units in which $\hbar=c=1$) which can be emitted is the same for all directions (hereafter we use the word "isotropic" in this sense) and is much less than m.

However, in Exp. II the photon can steal almost all the energy from $\bar{P}_2'$ (see Fig. 6) which is undetected; hence in the direction of $\bar{P}_2'$ the maximum energy of the photon $\bar{K}_{\max}$ is equal to $(\bar{E}_2')_{\text{elastic}}$, whereas in the backward direction it can be shown that $\bar{K}_{\max}\approx m\Delta\bar{\theta}/\bar{\theta}_{\text{elastic}}$ (see Fig. 6). Thus $\bar{K}_{\max}$ is neither isotropic nor $\ll m$.

In contrast to electron-nucleus scattering, the inelastic part of the radiative corrections to $e-e$ scattering (the same can be said about the Compton scattering) depends very critically upon the geometry of the experiment. (This is why we have specified the experimental conditions in such a detailed manner at the beginning of this section.) Recall that in the usual calculations of the radiative corrections to electron-nucleus scattering the following three conditions are assumed implicitly:

1. Due to the heavy mass of the nucleus, the real photons emitted by the nuclear current are negligible.
2. The energies of the elastically scattered electrons are not sharply dependent upon the scattering angles.
3. The momenta of recoil nuclei are not measured.

From these three conditions one can deduce the condition that the maximum energy of photons emitted is approximately isotropic irrespective of the shape and the size (if it is small) of the entrance slit and is equal to the energy resolution of the detecting system ΔE. ($\Delta E=E_{\text{elastic}}-E_{\min}$, where $E_{\min}$ is the threshold of the detecting system.) The three conditions are not satisfied in electron-electron scattering, either in Exp. I or Exp. II. In Exp. I the detecting system does not have any energy resolution since Čerenkov counters cannot distinguish between electrons with energies, say, ≈ 10 Mev and 500 Mev. Thus very hard photons (≈ 500 Mev) can be emitted along the directions of final electrons. The maximum energy of photons which can be emitted in other directions is a very complicated function of the geometry of the experiment and will be discussed in detail in Sec. III. The final expression for the cross section depends upon the half-angle of the detecting system $\Delta\theta$ (see Fig. 1). In Exp. II the energy resolution of the spectrometer $\Delta\bar{E}_1'$ is very small and it will be shown later that the radiative corrections for this experiment depend upon the quantity $\Delta\bar{\theta}$ (see Fig. 6) rather than the energy resolution of the spectrometer $\Delta\bar{E}_1'$.

Similar to Brown and Feynman's[5] result on the radiative corrections to Compton scattering, Redhead and Polovin's results contain terms like $\alpha\ln^2(-q^2/m^2)$ (compared with unity), which one does not find in the radiative corrections to electron-nucleus scattering[6] or large-angle pair production.[7] This kind of term is very undesirable because it is of order unity at high energies. If this kind of term really exists then it is indeed very serious since it implies that the power series expansion of the cross section in terms of α is no longer

[3] M. L. G. Redhead, Proc. Roy. Soc. (London) **A220**, 219 (1953).
[4] R. V. Polovin, J. Exptl. Theoret. Phys. (U.S.S.R.) **31**, 449 (1956) [translation: Soviet Phys.—JETP **4**, 385 (1957)].
[5] L. M. Brown and R. P. Feynman, Phys. Rev. **85**, 231 (1952).
[6] H. Suura, Phys. Rev. **99**, 1020 (1955).
[7] J. D. Bjorken, S. D. Drell, and S. C. Frautschi, Phys. Rev. **112**, 1409 (1958).

valid even at energies with which we are concerned here. Fortunately we found that the existence of terms like $\alpha \ln^2(-q^2/m^2)$ in references 3, 4, and 5 is due to those authors' special assumptions on $\bar{K}_{\max}$. In fact under the experimental conditions of Exp. I and Exp. II it will be shown later that these terms are associated with the infrared contribution and that they cancel out completely after addition of elastic and inelastic cross sections.

The notations used in this paper are similar to those used by Schweber *et al.*[8] The units $\hbar=c=1$ and $e^2/4\pi=\alpha$ are used. The relativistic notation used is such that $a_\mu(a_0,\mathbf{A})$, $a_\mu\gamma^\mu=\boldsymbol{a}$, $(a\cdot b)=a_0b_0-\mathbf{A}\cdot\mathbf{B}$, $\gamma_\mu\gamma_\nu+\gamma_\nu\gamma_\mu=2g_{\mu\nu}$, where $g_{00}=-g_{11}=-g_{22}=-g_{33}=1$ and all other g_{ij}'s are zero. p_1 and p_2 refer to 4-momenta associated with incoming electrons and p_1' and p_2' those with outgoing electrons.

The calculation of the cross sections can be separated into two parts: elastic and inelastic. Elastic parts refer to those diagrams which have two final electrons but no final photons. Inelastic parts refer to those diagrams which emit a photon in addition to the two outgoing electrons. Elastic and inelastic parts do not interfere with each other because they have different final states. The observable cross section is obtained by adding the elastic and inelastic cross sections.

We assume that a photon has a small mass λ whenever we deal with the processes which involve the emission of very soft (real or virtual) photons. This is just a device to avoid the so-called infrared divergence. In our calculation this method of infrared cutoff has many advantages over the alternative method which uses a noncovariant energy cutoff $K_{\min}$. If $K_{\min}$ is used as an infrared cutoff, the calculation for the inelastic parts for Exp. I can be slightly simplified, but the calculation for the elastic parts becomes extremely cumbersome. Moreover since $K_{\min}$ is noncovariant it is very inconvenient for performing a coordinate transformation. For example, had we used $K_{\min}$ instead of λ, we would have to calculate the elastic cross sections for Exp. I and Exp. II separately instead of obtaining one from the other by just a simple substitution.

When the fictitious photon mass λ is used as an infrared cutoff, the quantity λ always appears in the form $\ln(m/\lambda)$ in the self-energy diagrams (M_6) and in the forms $\mu_2(q^2)$, $\mu_2(q'^2)$, $\mu_2(-s^2)$ in other elastic infrared diagrams, where the function $\mu_2(q^2)$ is defined as

$$\mu_2(q^2)=\int_0^1 \frac{dy\,\ln[m^2\lambda^{-2}-y(1-y)q^2\lambda^{-2}]}{m^2-y(1-y)q^2-i\epsilon}$$
$$\approx\frac{-2}{q^2}\left[\ln\left(\frac{-q^2}{m^2}\right)\ln\left(\frac{m^2}{\lambda^2}\right)+\frac{1}{2}\ln^2\left(\frac{-q^2}{m^2}\right)-\frac{\pi^2}{6}\right]$$
$$(\text{for } -q^2\gg m^2).$$

[8] S. S. Schweber, H. A. Bethe, and F. de Hoffmann, *Mesons and Fields* (Row, Peterson and Company, Evanston, Illinois, 1955), Vol. I.

In the inelastic cross section one always finds similar terms but with a different sign. [In fact in our case the quantity λ appears in the direct two-photon exchange diagrams M_2 and $\tilde{M}_2$ as $\mu_2(s^2)$ rather than $\mu_2(-s^2)$, but this does not affect our argument since the imaginary part does not contribute to the cross section and we have neglected the nonlogarithmic terms in the calculation of two-photon exchange diagrams anyway.] Thus these terms cancel each other when elastic and inelastic terms are added together. Hence we shall call terms like $\ln(m/\lambda)$, $\mu_2(q^2)$, $\mu_2(q_1^2)$, and $\mu_2(-s^2)$ infrared terms.

In Sec. VI a preliminary study was made on the electron-positron colliding beam experiment. In the Appendix the vacuum polarizations involving heavier particles than an electron pair in the closed loop are investigated.

II. ELASTIC SCATTERING

Let us define $q=(p_1-p_1')$, $q'=(p_1-p_2')$, and $s=(p_1+p_2)$, where p_1' and p_2' refer to 4 momenta of outgoing electrons in the "elastic scattering." q and q' are space-like vectors and s is a time-like vector. For Exp. I we have

$$q^2=-4(E^2-m^2)\sin^2(\theta/2)\approx-4E^2\sin^2(\theta/2),$$
$$q'^2=-4(E^2-m^2)\cos^2(\theta/2)\approx-4E^2\cos^2(\theta/2),$$
$$s^2=4E^2,$$

where $E=E_1=E_2=E_1'=E_2'$. For Exp. II we have (denoting the laboratory quantities by a bar)

$$\bar{E}_2=m,$$
$$q^2=2m^2-2m\bar{E}_2'=-2m(\bar{E}_1-\bar{E}_1'),$$
$$q'^2=2m^2-2m\bar{E}_1'\approx-2m\bar{E}_1',$$
$$s^2=2m^2+2m\bar{E}_1\approx2m\bar{E}_1.$$

The following relations are useful:

$$q\cdot q'=q\cdot s=q'\cdot s=0,$$
$$q^2+q'^2+s^2=4m^2\approx0,$$
$$q\cdot p_1=q\cdot p_2'=-q\cdot p_2=-q\cdot p_1'=q^2/2,$$
$$q'\cdot p_1=q'\cdot p_1'=-q'\cdot p_2'=-q'\cdot p_2=q'^2/2,$$
$$s\cdot p_1=s\cdot p_2=s\cdot p_1'=s\cdot p_2'=s^2/2.$$

It should be noted that all the formulas given above hold only for elastic scattering, since in inelastic scattering p_1' and p_2' depend upon the photon 4-momentum k.

In either Exp. I or Exp. II we have s^2, $-q^2$, $-q'^2\gg m^2$. Thus in our calculation we neglect terms of order m^2/s^2, m^2/q^2, and m^2/q'^2 compared with 1. For simplicity we refer to them as $O(m^2/q^2)$. We shall call this kind of approximation the high-energy approximation. With the high-energy approximation the calculation can be simplified enormously. For example, the projection operator $(\boldsymbol{p}+m)/2m$ can be replaced by $\boldsymbol{p}/2m$ and $\boldsymbol{p}u(p)=mu(p)=0$.

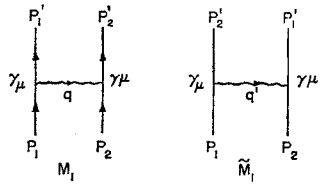

FIG. 2. Diagrams for Møller scattering.

The Feynman diagrams for the lowest order elastic electron-electron scattering (Møller scattering) are shown in Fig. 2, and those for the next order (elastic radiative corrections) are shown in Fig. 3. Self-energy diagrams M_6 do not have to be calculated explicitly since, for example, after mass renormalization $M_6(p_1)+M_6(p_1')$ cancels[9] out with M_5 taken at $q^2=0$. Thus we shall assume the vertex diagrams such as M_5 to be renormalized and forget about the self-energy diagrams such as M_6. We may write the elastic cross section as follows[10]:

$$\sigma_{\text{elastic}}=(2\pi)^2\frac{E_1E_2}{((p_1\cdot p_2)^2-m^4)^{\frac{1}{2}}}\frac{1}{4}\times\int\delta(p_1'+p_2'-p_1-p_2)d^3p_1'd^3p_2'\times\sum_{\text{spin}}[(M_1^\dagger M_1-\tilde{M}_1^\dagger M_1+\text{exchange})+\sum_{i=2}^{4}2\,\text{Re}(M_1^\dagger M_i-\tilde{M}_1^\dagger M_i+\text{exchange})+4\,\text{Re}(M_1^\dagger M_5-\tilde{M}_1^\dagger M_5+\text{exchange})], \quad (1)$$

where by "exchange" we mean the terms obtained by an interchange $p_1'\leftrightarrow p_2'$ or $q^2\leftrightarrow q'^2$. The factor 4 is associated with the vertex matrix element because, as will be shown later, in the high-energy approximation $M_5=M_5'$ and $\tilde{M}_5=\tilde{M}_5'$. We want to use Eq. (1) to calculate the elastic cross sections for both Exp. I and Exp. II. We notice that the factor

$$\sum_{\text{spin}}(M_1^\dagger M_i-\tilde{M}_1^\dagger M_i+\text{exchange}),\quad (i=1,\cdots,5)$$

is an invariant function times a factor $(E_1E_2E_1'E_2')^{-1}$. [See for example Eq. (2).] Thus the factors E_1E_2 in Eq. (1) cancel out and we have the remaining final-state integration,

$$A=\int\delta(p_1'+p_2'-p_1-p_2)\frac{d^3p_1'}{E_1'}\frac{d^3p_2'}{E_2'},$$

whose range of integration is subject to the experimental conditions. For Exp. I this integration reduces to

$$A_{\text{I}}=d\Omega_1'\int P_1'dE_1'\int\delta(p_1'+p_2'-s)2\theta(E_2')\times\delta(p_2'^2-m^2)d^4p_2'=d\Omega_1'\int 2P_1'\delta((s-p_1')^2-m^2)dE_1'=\frac{P_1'}{2E}d\Omega_1'\approx d\Omega_1'/2.$$

For Exp. II the elastic cross section depends upon the energy resolution $\Delta\bar{E}_1'$ of the spectrometer rather than the width of the entrance slit; thus we have

$$A_{\text{II}}=\bar{P}_1'\Delta\bar{E}_1'\int d\bar{\Omega}_1'\,2\delta(s^2-2p_1'\cdot s)=\bar{P}_1'\Delta\bar{E}_1'\int\frac{a}{D}d\bar{\theta}\times2\delta(s^2-2m\bar{E}_1'-2E_1E_1'+2\bar{P}_1\bar{P}_1'\cos\bar{\theta})=\frac{a}{D}\frac{\Delta\bar{E}_1'}{\bar{P}_1\sin\bar{\theta}_{\text{elastic}}},$$

where D is the distance between the scattering region and the entrance slit and a is the width of the entrance slit measured perpendicular to the θ direction (see Fig. 6). Thus the expression for the elastic cross section of Exp. II can be obtained from that of Exp. I by a simple substitution of the factor $A_{\text{I}}\rightarrow A_{\text{II}}$.

The terms $M_1^\dagger M_1-M_1^\dagger M_1+\text{exchange}$ in Eq. (1) represent the Møller scattering. The matrix element for the Møller scattering is

$$M_1-\tilde{M}_1=c_M[q^{-2}\bar{u}(p_1')\gamma_\mu u(p_1)\bar{u}(p_2')\gamma^\mu u(p_2)-q'^{-2}\bar{u}(p_2')\gamma_\mu u(p_1)\bar{u}(p_1')\gamma^\mu u(p_2)], \quad (2)$$

where $c_M=i\alpha\pi^{-1}m^2(E_1E_1'E_2E_2')^{-\frac{1}{2}}$. After averaging over the initial states and summing over the final states,

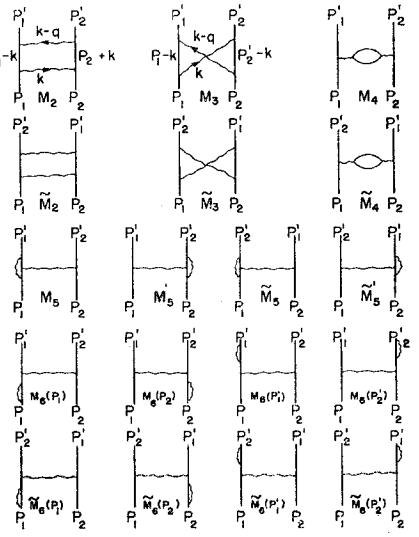

FIG. 3. Diagrams for elastic radiative corrections.

[9] R. P. Feynman, Phys. Rev. **76**, 769 (1949).

[10] For the expression of cross sections in the invariant form, see J. M. Jauch and F. Rohrlich, *Theory of Photons and Electrons* (Addison-Wesley Publishing Company, Inc., Reading, Massachusetts, 1955), Eq. (8-49).

the cross section for the Møller scattering for Exp. I in the high-energy approximation is

$$d\sigma^{\mathrm{I}}_{\mathrm{M\o ller}}=\frac{r_0^2}{8}\frac{m^2}{E^2}d\Omega_1'\left[\frac{s^4+q'^4}{q^4}+\frac{2s^4}{q^2q'^2}+\frac{s^4+q^4}{q'^4}\right], \quad (3)$$

where $r_0=\alpha/m\sim 2.82\times 10^{-13}$ cm is the classical radius of an electron. Similarly the Møller cross section for Exp. II is

$$d\sigma^{\mathrm{II}}_{\mathrm{M\o ller}}=\frac{r_0^2}{2}\frac{m}{\bar{E}_1^2}\frac{a\Delta\bar{E}_1'}{D\sin\bar{\theta}_{\mathrm{elastic}}}\times\left[\frac{s^4+q'^4}{q^4}+\frac{2s^4}{q^2q'^2}+\frac{s^4+q^4}{q'^4}\right]. \quad (4)$$

The vacuum polarization and the vertex diagrams are calculated using the method of Feynman.[9] After charge renormalization, the matrix element for the vacuum polarization diagram M_4 can be written as

$$M_4=\frac{\alpha}{\pi}\left[\frac{-5}{9}+\frac{1}{3}\ln\left(\frac{-q^2}{m^2}\right)\right]M_1. \quad (5)$$

The vacuum polarizations due to heavier particles than an electron pair in the closed loop are discussed in the Appendix.

The matrix element for the vertex diagram M_5 after renormalization can be written as

$$M_5=-\frac{\alpha}{2\pi}\left[-\frac{q^2}{2}\mu_2(q^2)-\ln\left(\frac{m^2}{\lambda^2}\right)-\frac{3}{2}\ln\left(\frac{-q^2}{m^2}\right)+2\right]M_1+\frac{\alpha}{2\pi}M_A, \quad (6)$$

where

$$M_A=\frac{c_M}{2}\frac{m}{q^4}\ln\left(\frac{-q^2}{m^2}\right)\bar{u}(p_1')(q\gamma_\mu-\gamma_\mu q)\times u(p_1)\bar{u}(p_2')\gamma^\mu u(p_2),$$

$$\mu_2(q^2)=-\frac{2}{q^2}\left[\ln\left(\frac{-q^2}{m^2}\right)\ln\left(\frac{m^2}{\lambda^2}\right)+\frac{1}{2}\ln^2\left(\frac{-q^2}{m^2}\right)-\frac{\pi^2}{6}\right]. \quad (7)$$

M_A is the anomalous magnetic moment term and as can be readily seen this term is negligible, namely of order $O(m^2/q^2)$. The matrix element for M_5' can be obtained from M_5 by the interchange $p_1\leftrightarrow p_2$, $p_1'\leftrightarrow p_2'$ and $q\leftrightarrow -q$. Since the anomalous magnetic moment term is negligible and the rest of the matrix element is invariant under this interchange, we have $M_5\approx M_5'$. Thus $M_5+M_5'\approx 2M_5$. This explains the factor 4 associated with M_5 in Eq. (1). $\mu_2(q^2)$ is the infrared contribution of the vertex diagram M_5 before the renormalization and $\ln(m^2/\lambda^2)$ in Eq. (6) comes from the infrared contribution of the self energy diagrams $M_6(p_1)+M_6(p_1')$. Both of these infrared terms cancel out with the corresponding infrared terms from the bremsstrahlung. Thus after infrared cancellation M_5 can be written as

$$M_5\rightarrow -\frac{\alpha}{2\pi}\left[2-\frac{3}{2}\ln\left(\frac{-q^2}{m^2}\right)\right]M_1. \quad (8)$$

The two-photon exchange diagrams M_2 and M_3 are the most difficult to calculate of all the diagrams. We notice in both diagrams that when $k\rightarrow 0$ or $k-q\rightarrow 0$ we have infrared divergence. The evaluation of the noncrisscross two-photon exchange diagram M_2 is slightly more complicated than the crisscross two-photon exchange diagram M_3, because in M_2 the intermediate state can become real; thus we have to cross a pole in the path of integration with respect to k. The path of integration around the pole is taken care of by assuming that m and λ have small negative imaginary parts, $m\rightarrow m-i\epsilon$, $\lambda\rightarrow\lambda-i\epsilon'$. The matrix element for M_2 can be written as

$$M_2=\frac{e^4}{(2\pi)^6}\frac{m^2}{(E_1E_2E_1'E_2')^{\frac{1}{2}}}\left[4(p_1\cdot p_2)(\gamma_\mu\times\gamma^\mu)b+2\{(\gamma_\mu\gamma^\sigma p_2\times\gamma^\mu)-(\gamma_\mu\times\gamma^\mu\gamma^\sigma p_1)\}b_\sigma-(\gamma_\mu\gamma^\sigma\gamma_\nu\times\gamma^\mu\gamma^\tau\gamma^\nu)b_{\sigma\tau}\right], \quad (9)$$

where $(A\times B)\equiv\bar{u}(p_1')Au(p_1)\bar{u}(p_2')Bu(p_2)$, and

$$(b;b_\sigma;b_{\sigma\tau})=\int\frac{(1;k_\sigma;k_\sigma k_\tau)d^4k}{(k^2-2p_1\cdot k)(k^2+2k\cdot p_2)(k^2-\lambda^2)\{(k-q)^2-\lambda^2\}}. \quad (10)$$

The matrix element for M_3 can be written as

$$M_3=\frac{e^4}{(2\pi)^6}\frac{m^2}{(E_1E_2E_1'E_2')^{\frac{1}{2}}}\left[4(p_1p_2')(\gamma_\mu\times\gamma^\mu)c-2\{(\gamma_\mu\gamma^\sigma p_2'\times\gamma^\mu)+(\gamma_\mu\times p_1\gamma^\sigma\gamma^\mu)\}c_\sigma+(\gamma_\mu\gamma^\sigma\gamma_\nu\times\gamma^\nu\gamma^\tau\gamma^\mu)c_{\sigma\tau}\right], \quad (11)$$

where

$$(c;c_\sigma;c_{\sigma\tau})=\int\frac{(1;k_\sigma;k_\sigma k_\tau)d^4k}{(k^2-2p_1\cdot k)(k^2-2k\cdot p_2')(k^2-\lambda^2)\{(k-q)^2-\lambda^2\}}. \quad (12)$$

From Eqs. (10) and (12) we see that $(b;b_\sigma;b_{\sigma\tau})$ can be obtained from $(c;c_\sigma;c_{\sigma\tau})$ by an interchange of $p_2'\leftrightarrow -p_2$. The interchange of $p_2'\leftrightarrow -p_2$ is equivalent

to $s^2 \leftrightarrow q'^2$. Equation (12) is easier to calculate than Eq. (10) since there is no real intermediate state in M_3, hence no poles in the region of integration in Eq. (12). We have calculated Eqs. (10) and (12) independently and the results verify the above observation. In applying the above substitution we notice the following. Suppose in Eq. (12) we obtain a quantity like $\ln(-q'^2/m^2)$. After the substitution $p_2' \leftrightarrow -p_2$ we get $\ln(-s^2/m^2) = \ln(s^2/m^2) \pm \pi i$. The sign of the imaginary part cannot be determined unless we actually carry out the integration of Eq. (10). However, the imaginary part does not contribute to the cross section due to Eq. (1), hence the ambiguity in the sign of the imaginary part does not give any trouble. Due to the complexity involved in the integrations of Eqs. (10) and (12) we neglect nonlogarithmic terms in the calculation. Using the method similar to the one used in reference 3, we can evaluate $(c; c_\sigma; c_{\sigma\tau})$ and the results are as follows:

$$c=\frac{2\pi^2 i}{q^2 q'^2}\ln\left(\frac{-q^2}{\lambda^2}\right)\ln\left(\frac{-q'^2}{m^2}\right),$$

$$c_\sigma = X(p_1+p_2')_\sigma + Yq_\sigma,$$

where

$$X=\frac{\pi^2 i}{2q'^2}\left[\frac{1}{q^2}\ln^2\left(\frac{-q^2}{m^2}\right)+\frac{1}{s^2}\ln^2\left(\frac{-q'^2}{-q^2}\right)\right],$$

$$Y=-X+c=\frac{\pi^2 i}{2q^2 s^2}\ln^2\left(\frac{-q'^2}{-q^2}\right)-\frac{\pi^2 i}{2q^2}\mu_2(q'^2),$$

$$c_{\sigma\tau}=(p_1+p_2')_\sigma(p_1+p_2')_\tau K+(p_1-p_2')_\sigma(p_1-p_2')_\tau L$$
$$+[(p_1+p_2')_\sigma q_\tau+q_\sigma(p_1+p_2')_\tau]W+q_\sigma q_\tau Z+g_{\sigma\tau}T,$$

where

$$K=\frac{\pi^2 i}{-2s^2}\left\{\mu_1(q^2)+\mu_1(q'^2)+\frac{1}{q^2}\ln^2\left(\frac{-q^2}{m^2}\right)\right\}+\frac{(q'^2-q^2)}{2s^2}X,$$

$$L=\frac{X}{2}+\frac{\pi^2 i}{2q'^2}\mu_1(q^2),$$

$$W=\frac{-q'^2}{s^2}X+\frac{\pi^2 i}{2s^2}\left\{\mu_1(q^2)+\mu_1(q'^2)+\frac{1}{q^2}\ln^2\left(\frac{-q^2}{m^2}\right)\right\},$$

$$Z=\frac{-q'^4 X}{q^2 s^2}+\frac{\pi^2 i}{2q^2}\left\{\frac{-q^2}{s^2}\mu_1(q^2)+\left(2+\frac{q'^2}{s^2}\right)\mu_1(q'^2)-\mu_2(q'^2)+\frac{q'^2}{s^2 q^2}\ln^2\left(\frac{-q^2}{m^2}\right)\right\},$$

$$T=-\frac{\pi^2 i}{4s^2}\ln^2\left(\frac{-q'^2}{-q^2}\right),$$

$$\mu_1(q^2)=\int_0^1 \frac{dy}{m^2-(1-y)yq^2-i\epsilon}\approx\frac{-2}{q^2}\ln\left(\frac{-q^2}{m^2}\right).$$

Substituting the values of c, c_σ, and $c_{\sigma\tau}$ in Eq. (11), we can simplify the expression for M_3 as follows:

$$M_3=\frac{e^4}{(2\pi)^6}\frac{m^2\pi^2 i}{(E_1E_2E_1'E_2')^{\frac{1}{2}}}\left\{(\gamma_\mu\times\gamma^\mu)\left[\frac{2q'^2}{q^2}\mu_2(q'^2)+\frac{q'^2(q^2-2s^2)}{q^2s^4}\ln^2\left(\frac{-q'^2}{-q^2}\right)+\frac{2(s^2-q'^2)}{q^2s^2}\ln\left(\frac{-q'^2}{-q^2}\right)\right]\right.$$
$$+(\boldsymbol{p}_2'\times\boldsymbol{p}_1)\frac{4}{s^2}\left[\frac{1}{s^2}\ln^2\left(\frac{-q'^2}{-q^2}\right)-\frac{2}{q^2}\ln\left(\frac{-q'^2}{-q^2}\right)\right]+(\gamma_\mu\boldsymbol{p}_2'\gamma_\nu\times\gamma^\nu\boldsymbol{p}_1\gamma^\mu)\frac{1}{s^2}\left[\frac{1}{2s^2}\ln^2\left(\frac{-q'^2}{-q^2}\right)+\frac{1}{q'^2}\ln\left(\frac{-q'^2}{-q^2}\right)\right]$$
$$\left.-(\gamma_\mu\gamma_\sigma\gamma_\nu\times\gamma^\nu\gamma^\sigma\gamma^\mu)\frac{1}{4s^2}\ln^2\left(\frac{-q'^2}{-q^2}\right)\right\}. \quad (13)$$

The fact that M_3 can be decomposed into a linear combination of only 4 spinor matrix elements[11] greatly simplifies the calculation. For example, in the calculation of spin sum of $M^\dagger M_3 - M_1^\dagger \tilde{M}_3$ in Eq. (1), one has to take only 8 traces instead of 42 traces. Similarly, the matrix element M_2 can be written as

$$M_2=\frac{e^4}{(2\pi)^6}\frac{m^2\pi^2 i}{(E_1E_2E_1'E_2')^{\frac{1}{2}}}\left\{-(\gamma_\mu\times\gamma^\mu)\left[\frac{2s^2}{q^2}\mu_2(s^2)+\frac{s^2(q^2-2q'^2)}{q^2q'^4}\ln^2\left(\frac{-s^2}{-q^2}\right)+\frac{2(q'^2-s^2)}{q^2q'^2}\ln\left(\frac{-s^2}{-q^2}\right)\right]\right.$$
$$+(\boldsymbol{p}_2\times\boldsymbol{p}_1)\frac{4}{q'^2}\left[\frac{1}{q'^2}\ln^2\left(\frac{-s^2}{-q^2}\right)-\frac{2}{q^2}\ln\left(\frac{-s^2}{-q^2}\right)\right]+(\gamma_\mu\boldsymbol{p}_2\gamma_\nu\times\gamma^\mu\boldsymbol{p}_1\gamma^\nu)\frac{1}{q'^2}\left[\frac{1}{2q'^2}\ln^2\left(\frac{-s^2}{-q^2}\right)+\frac{1}{s^2}\ln\left(\frac{-s^2}{-q^2}\right)\right]$$
$$\left.+(\gamma_\mu\gamma_\sigma\gamma_\nu\times\gamma^\mu\gamma^\sigma\gamma^\nu)\frac{1}{4q'^2}\ln^2\left(\frac{-s^2}{-q^2}\right)\right\}. \quad (14)$$

[11] This was pointed out to the author by Professor D. R. Yennie.

The resemblance between Eqs. (13) and (14) should be noted. In fact all the coefficients of the spinor matrix elements in the two expressions are related by the simple substitution $p_2' \leftrightarrow -p_2$ or $q'^2 \leftrightarrow s^2$.

After taking the spin sum we obtain the following expressions:

$$\sum_{\text{spin}} 2\,\mathrm{Re}(M_1^\dagger M_2 - \tilde{M}^\dagger M_2) = \frac{2\alpha}{\pi}\sum_{\text{spin}}[M_1^\dagger M_1 - \tilde{M}_1^\dagger M_1]\frac{s^2}{2}\mu_2(-s^2) - \frac{\alpha^3}{2\pi^3 E_1 E_2 E_1' E_2'}\left\{\left[\frac{3s^4+q'^4}{2q^4}+\frac{s^4}{q^2q'^2}\right]\ln^2\left(\frac{s^2}{-q^2}\right)-\frac{q'^2}{q^2}\ln\left(\frac{s^2}{-q^2}\right)\right\}, \quad (15)$$

$$\sum_{\text{spin}} 2\,\mathrm{Re}(M_1^\dagger M_3 - \tilde{M}_1^\dagger M_3) = \frac{2\alpha}{\pi}\sum_{\text{spin}}[M_1^\dagger M_1 - \tilde{M}_1^\dagger M_1]\frac{q'^2}{2}\mu_2(q'^2) + \frac{\alpha^3}{2\pi^3 E_1 E_2 E_1' E_2'}\left\{\left[\frac{3q'^4+s^4}{2q^4}+\frac{s^4+q'^4}{2q^2q'^2}\right]\ln^2\left(\frac{-q'^2}{-q^2}\right)+\frac{s^4}{q^2q'^2}\ln\left(\frac{-q'^2}{-q^2}\right)\right\}. \quad (16)$$

$\mu_2(-s^2)$ and $\mu_2(q'^2)$ are associated with infrared and it will be shown later that they cancel out with the similar terms in the soft real photon cross section. Substituting Eqs. (5), (6) (with M_A neglected), (15), and (16) into Eq. (1), and using (3), we can write the expression for the elastic cross section for Exp. I as follows:

$$d\sigma^{\mathrm{I}}_{\text{elastic}} = \frac{r_0^2}{8}\frac{m^2}{E^2}d\Omega_1'\left\{\left(\frac{s^4+q'^4}{q^4}+\frac{s^4}{q'^2q^2}\right)\left[1-\frac{4\alpha}{\pi}\left(\frac{23}{18}-\frac{11}{12}\ln\left(\frac{-q^2}{m^2}\right)\right)\right]+\text{exchange}+\frac{\alpha}{\pi}[f(x)+f(1-x)]\right\} + d\sigma^{\mathrm{I}}_{\text{Møller}}\frac{\alpha}{\pi}\left[4\ln\left(\frac{m}{\lambda}\right)+s^2\mu_2(-s^2)+q^2\mu_2(q^2)+q'^2\mu_2(q'^2)\right], \quad (17)$$

where

$$f(x) = -\left(\frac{3s^4+q'^4}{2q^4}+\frac{s^4}{q^2q'^2}\right)\ln^2\left(\frac{s^2}{-q^2}\right)+\frac{q'^2}{q^2}\ln\left(\frac{s^2}{-q^2}\right)+\left(\frac{3q'^4+s^4}{2q^4}+\frac{s^4+q'^4}{2q^2q'^2}\right)\ln^2\left(\frac{-q'^2}{-q^2}\right)+\frac{s^4}{q^2q'^2}\ln\left(\frac{-q'^2}{-q^2}\right)$$

$$= -\left(\frac{3+(1-x)^2}{2x^2}+\frac{1}{x(1-x)}\right)\ln^2\left(\frac{1}{x}\right)+\frac{1-x}{x}\ln\left(\frac{1}{x}\right) + \left(\frac{3(1-x)^2+1}{2x^2}+\frac{1+(1-x)^2}{2x(1-x)}\right)\ln^2\left(\frac{(1-x)}{x}\right)+\frac{1}{x(1-x)}\ln\left(\frac{(1-x)}{x}\right),$$

$$x = \frac{-q^2}{s^2} = \sin^2(\theta/2).$$

$f(x)+f(1-x)$ is the contribution from the two-photon exchange diagrams after infrared cancellation. It is very important to notice that its contribution to the cross section is negligible, namely 0.1, 0.03 and 0 percent, respectively, at $\theta=90°$, 35°, and 0°. It is also interesting to notice that from Eq. (15) and Eq. (16) the noncrisscross and crisscross two-photon exchange terms do not go to zero separately in the forward or backward direction. However their sum, aside from the infrared terms μ_2 which cancel out eventually, does have this desirable feature. In fact M_2 or M_3 alone is not gauge invariant but their sum is. The property of gauge invariance can be demonstrated easily by replacing γ_ν in M_2 and M_3 by $k^\nu\gamma_\nu$. Thus one would not expect the noncrisscross or the crisscross two-photon exchange terms separately to have any physical meaning but one should expect their sum to be meaningful. The terms in the last bracket of Eq. (17) represent the infrared terms which cancel out with the infrared terms of the soft real photon cross section [see Eq. (22)].

The elastic cross section $d\sigma^{\mathrm{II}}_{\text{elastic}}$ for Exp. II can be obtained from Eqs. (3), (4), and (17); and we have

$$d\sigma^{\mathrm{II}}_{\text{elastic}} = \frac{r_0^2}{2}\frac{m}{\bar{E}_1^2}\frac{a\Delta\bar{E}_1'}{D\sin\bar{\theta}_{\text{elastic}}}\left\{\left(\frac{s^4+q'^4}{q^4}+\frac{s^4}{q'^2q^2}\right)\times\left[1-\frac{4\alpha}{\pi}\left(\frac{23}{18}-\frac{11}{12}\ln\left(\frac{-q^2}{m^2}\right)\right)\right] +\text{exchange}+\frac{\alpha}{\pi}[f(x)+f(1-x)]\right\} + d\sigma^{\mathrm{II}}_{\text{Møller}}\frac{\alpha}{\pi}\left[4\ln\left(\frac{m}{\lambda}\right)+s^2\mu_2(-s^2)+q^2\mu_2(q^2)+q'^2\mu_2(q'^2)\right]. \quad (18)$$

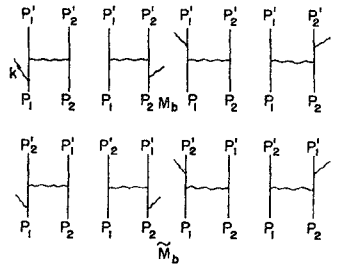

FIG. 4. Diagrams for inelastic radiative corrections.

Here again $f(x)+f(1-x)$ can be neglected and it will be shown in Sec. V that the terms in the last bracket in Eq. (18) represent the infrared contribution and cancel out with the infrared contribution of the inelastic cross section [see Eq. (52)].

III. INELASTIC SCATTERING FOR EXP. I

A. Soft Photon Cross Section

The diagrams associated with inelastic $e-e$ scattering are shown in Fig. 4. The matrix elements for these processes can be written as $M_b-\tilde{M}_b$ where

$$M_b=\frac{e^3}{(2\pi)^{\frac{3}{2}}}\frac{m^2}{(2\omega E_1E_2E_1'E_2')^{\frac{1}{2}}}\times\left[\frac{(c^\mu(p_1',p_1)\times\gamma_\mu)}{(p_2'-p_2)^2}+\frac{(\gamma_\mu\times c^\mu(p_2',p_2))}{(p_1-p_1')^2}\right], \quad (19)$$

$$c^\mu(p_1',p_1)=\left(\frac{p_1'\cdot e}{p_1'\cdot k}-\frac{p_1\cdot e}{p_1\cdot k}\right)\gamma_\mu+\frac{1}{2}\left(\frac{e\!\!\!/k\gamma_\mu}{p_1'\cdot k}+\frac{\gamma_\mu k\!\!\!/e}{p_1\cdot k}\right). \quad (20)$$

e is the polarization vector of the photon emitted. $\tilde{M}_b$ is obtained from M_b by the interchange of $p_1'\leftrightarrow p_2'$. The inelastic cross section can be written as:

$$d\sigma_{\text{inelastic}}=(2\pi)^2\frac{E_1E_2}{[(p_1\cdot p_2)^2-m^4]^{\frac{1}{2}}}\frac{1}{4}\times\int\delta(p_1'+p_2'+k-p_1-p_2)d^3p_1'd^3p_2'd^3k\times\sum_{\text{spin}}(M_b^\dagger M_b-\tilde{M}_b^\dagger M_b-M_b^\dagger\tilde{M}_b+\tilde{M}_b^\dagger\tilde{M}_b), \quad (21)$$

where $\sum_{\text{spin}}$ is the summation over electron spins and photon polarizations. Equations (19), (20), and (21) are true either for Exp. I or Exp. II. However the integration with respect to the final states is different for different experimental conditions. In this section we treat Exp. I. The inelastic cross section for Exp. I can be calculated most conveniently by separating the photons into soft and hard photons, depending upon the photon energy. From the denominators of Eq. (20) it can be readily seen that most photons are emitted in the directions along either p_1, p_2, p_1', or p_2'. From the δ function in Eq. (21) and the condition of coincidence of p_1' and p_2', it can be shown that the maximum energy of photon $K_{\max}$ which can be emitted along the directions of either p_1 or p_2 is $\Delta E\equiv 2E\Delta\theta/(\sin\theta+\Delta\theta)$, where $\Delta\theta$ is the half-angle of the Čerenkov counter. Similarly along p_1' or p_2' directions, the maximum energy of photon $K_{\max}$ is approximately equal to the incident energy of the electron E, since we have assumed that the Čerenkov counters do not have any energy resolution. Thus for convenience we define those photons having energy smaller than ΔE as soft photons and others as hard photons. The photon four-momentum k in the δ function of Eq. (21) and in the numerator of Eq. (20) can be neglected for soft photons. The neglect of k in the δ function implies two things; firstly the energy-momentum conservation for the elastic scattering, $p_1+p_2=p_1'+p_2'$, holds approximately, and secondly the maximum energy of photons which can be emitted is isotropic (the same for all directions) for each value of the electron scattering angle θ and is defined to be equal to $\Delta E=2E\Delta\theta/(\sin\theta+\Delta\theta)$. The infrared divergence which occurs in the soft photon cross section is avoided by assuming that a photon has a small mass λ. Designating the cross section associated with the emission of soft photons as $d\sigma_{\text{soft}}$, we obtain from Eq. (21)

$$d\sigma^{\text{I}}_{\text{soft}}=-d\sigma^{\text{I}}_{\text{Møller}}\frac{\alpha}{4\pi^2}\int_0^{\Delta E}\frac{k^2dk}{(k^2+\lambda^2)^{\frac{1}{2}}}\times\int d\Omega_K\left[\frac{4m^2}{(p_1\cdot k)^2}+\frac{4(p_1\cdot p_2)}{(p_1\cdot k)(p_2\cdot k)}-\frac{4(p_1\cdot p_1')}{(p_1\cdot k)(p_1'\cdot k)}-\frac{4(p_1\cdot p_2')}{(p_1\cdot k)(p_2'\cdot k)}\right]$$

$$=-d\sigma^{\text{I}}_{\text{Møller}}\frac{4\alpha}{\pi}\left\{\ln\left(\frac{E}{\Delta E}\right)\left[\ln\left(\frac{q^2q'^2}{s^2m^2}\right)-1\right]+\frac{1}{4}\left[4\ln\left(\frac{m}{\lambda}\right)+s^2\mu_2(-s^2)+q^2\mu_2(q^2)+q'^2\mu_2(q'^2)\right]\right\}. \quad (22)$$

From Eqs. (17) and (22), neglecting $f(x)+f(1-x)$, we have

$$d\sigma^{\text{I}}_{\text{elastic}}+d\sigma^{\text{I}}_{\text{soft}}=d\Omega_1'\frac{r_0^2}{8}\frac{m^2}{E^2}\left(\frac{s^4+q'^4}{q^4}+\frac{s^4}{q'^2q^2}\right)\times\left\{1-\frac{4\alpha}{\pi}\left[\frac{23}{18}-\frac{11}{12}\ln\left(\frac{-q^2}{m^2}\right)+\ln\left(\frac{E}{\Delta E}\right)\left(\ln\left(\frac{q^2q'^2}{s^2m^2}\right)-1\right)\right]\right\}$$

$$+\text{ terms obtained by interchange } q^2\leftrightarrow q'^2. \quad (23)$$

Thus we have achieved the infrared cancellation between elastic and inelastic cross sections. For $\theta \leqslant 90°$, Eq. (23) can be written approximately as

$$(d\sigma^{\mathrm{I}}{}_{\mathrm{elastic}}+d\sigma^{\mathrm{I}}{}_{\mathrm{soft}})_{\theta\leqslant 90°} \approx d\sigma^{\mathrm{I}}{}_{\mathrm{M\o ller}}\left\{1-\frac{4\alpha}{\pi}\left[\frac{23}{18}-\frac{11}{12}\ln\left(\frac{-q^2}{m^2}\right)+\ln\left(\frac{E}{\Delta E}\right)\left(\ln\left(\frac{q^2q'^2}{s^2m^2}\right)-1\right)\right]\right\}, \quad (24)$$

where $\Delta E=2E\Delta\theta/(\sin\theta+\Delta\theta)$.

The cross section given by Eq. (24) is about 0 and 0.17% smaller than that given by Eq. (23) at θ equal to 90° and 35°, respectively. It is interesting to notice the resemblance between Eq. (24) and the Schwinger radiative corrections[12] to potential scattering. In fact if we replace $\ln(q^2q'^2/s^2m^2)$ in Eq. (24) by $\ln(-q^2/m^2)$, the radiative correction terms in Eq. (24) are exactly the same as Schwinger's formula with the contributions from bremsstrahlung and vertex parts doubled but the vacuum polarization term undoubled. This is because in Schwinger's corrections the radiative corrections to the proton current are neglected, whereas in electron-electron scattering the radiative corrections to either of the electrons are equally important. This argument is valid because we have proved that the two-photon exchange diagrams contribute negligibly to the cross section after the infrared cancellation.

B. Hard-Photon Cross Section

In Sec. III A we have taken care of those photons which have energy smaller than ΔE and the infrared cancellation between elastic and inelastic cross sections. Here we consider those photons which have energy greater than ΔE and are emitted by the outgoing electrons p_1' and p_2'. The exact evaluation of the hard photon cross section is extremely complicated for two reasons. First, since k in the numerator of Eq. (20) can no longer be neglected, one has to take more than 100 traces of the γ matrices with each trace yielding half a dozen terms or more; secondly, k in the δ function of Eq. (21) is also no longer negligible, thus the maximum energy of the photons which can be emitted is no longer isotropic but depends very critically upon the direction in which they are emitted, and the magnitudes and directions of the 4 momenta of outgoing electrons p_1' and p_2' also depend upon the magnitude and the direction of k. However, if we neglect terms which are small compared with $\alpha\ln(E^2/m^2)$ and $\alpha\ln(E/\Delta E)$, we can simplify the calculation enormously. We shall call terms small compared with $\alpha\ln(E^2/m^2)$ and $\alpha\ln(E/\Delta E)$ nonlogarithmic terms and we shall neglect them in the calculation of hard-photon cross sections. Since most photons tend to be emitted along the directions of motion of the electrons from which they are emitted, we can infer that hard photons are emitted mainly from the final electrons p_1' and p_2' for reasons mentioned in Sec. III A. Thus we divide the hard-photon cross section into two parts, hard-photon emissions by p_1' and by p_2'. The two parts should be equal by the geometrical symmetry of the experiment. If photons are emitted by p_1', then the most significant terms in the matrix element are those terms with a denominator $p_1'\cdot k$, and all other terms can be approximated by assuming that photons are emitted in the direction of p_1'. Thus we have

$$k=p_1'\omega/E_1', \quad E_1'=E-\omega,$$
$$p_1\cdot k=E\omega(1-\cos\theta)=-q^2\omega/2E, \quad p_2\cdot k=-q'^2\omega/2E,$$
$$p_2'\cdot k=s^2\omega/2E, \quad p_1\cdot p_1'=-q^2E_1'/2E,$$
$$p_2\cdot p_1'=-q'^2E_1'/2E, \quad p_2'\cdot p_1'=s^2E_1'/2E,$$

and Eq. (19) can be written as

$$M_b=\frac{e^3}{(2\pi)^{7/2}}\frac{m^2}{(2\omega E_1E_2E_1'E_2')^{\frac{1}{2}}}\frac{1}{q^2}\left\{\left[\frac{p_1'\cdot e}{p_1'\cdot k}+\frac{2E(p_1\cdot e)}{q^2\omega}\right](\gamma_\mu\times\gamma^\mu)+\frac{\omega}{E_1'}\left[\frac{(\boldsymbol{e}\boldsymbol{p}_1'\gamma_\mu\times\gamma^\mu)}{2(p_1'\cdot k)}-\frac{E}{q^2\omega}(\gamma_\mu\boldsymbol{p}_1'\boldsymbol{e}\times\gamma^\mu)\right]\right.$$
$$\left.+\frac{2E^2}{E_1'}\left[\frac{p_2'\cdot e}{s^2\omega}+\frac{p_2\cdot e}{q'^2\omega}\right](\gamma_\mu\times\gamma^\mu)+\left(\frac{E}{E_1'}\right)^2\left[\frac{(\gamma^\mu\times\boldsymbol{e}\boldsymbol{p}_1'\gamma_\mu)}{s^2}-\frac{(\gamma^\mu\times\gamma_\mu\boldsymbol{p}_1'\boldsymbol{e})}{q'^2}\right]\right\}. \quad (25)$$

Similarly,

$$\tilde{M}_b=\frac{e^3}{(2\pi)^{7/2}}\frac{m^2}{(2\omega E_1E_2E_1'E_2')^{\frac{1}{2}}}\frac{1}{q'^2}\left\{\left[\frac{p_1'\cdot e}{p_1'\cdot k}+\frac{2E(p_2\cdot e)}{q'^2\omega}\right](\gamma_\mu\times\gamma^\mu)'+\frac{\omega}{E_1'}\left[\frac{(\gamma_\mu\times\boldsymbol{e}\boldsymbol{p}_1'\gamma^\mu)'}{2(p_1'\cdot k)}-\frac{E(\gamma_\mu\times\gamma^\mu\boldsymbol{p}_1'\boldsymbol{e})'}{q'^2\omega}\right]\right.$$
$$\left.+\frac{2E^2}{E_1'}\left[\frac{p_2'\cdot e}{s^2\omega}+\frac{p_1\cdot e}{q^2\omega}\right](\gamma_\mu\times\gamma^\mu)'+\left(\frac{E}{E_1'}\right)^2\left[\frac{(\boldsymbol{e}\boldsymbol{p}_1'\gamma_\mu\times\gamma^\mu)'}{s^2}-\frac{(\gamma_\mu\boldsymbol{p}_1'\boldsymbol{e}\times\gamma^\mu)'}{q^2}\right]\right\}, \quad (26)$$

where

$$(A\times B)'\equiv\bar{u}(p_2')Au(p_1)\bar{u}(p_1')Bu(p_2).$$

Before taking the summation over the electron spins and photon polarizations, we want to determine what kinds of terms in the integrand of Eq. (21) contribute

[12] J. Schwinger, Phys. Rev. **76**, 790 (1949), Eq. (2.105).

to logarithmic terms after the integration. To do this, we first simplify the expression

$$\int \frac{d^3p_1'}{E_1'}\int \frac{d^3p_2'}{E_2'}\int \frac{d^3k}{2\omega}\delta(p_1'+p_2'+k-p_1-p_2). \quad (27)$$

The only experimental condition which restricts the range of this integration is that the directions of p_1' and p_2' must be within the solid angles of the respective counters. After the integration with respect to p_1' and p_2' by using the δ function, this experimental condition is transformed into a restriction on the range of k integration. In the following we appeal to intuition and geometry to help determine the range of the k integration. We consider what kind of photon can be emitted by p_1' such that p_1' and p_2' are simultaneously detected by the respective counters. Figure 5 shows the geometry needed to determine the range of k integration. Suppose a photon k is emitted with an angle ψ from p_1' such that p_2' is barely accepted by the counter 2, hitting a point B on the periphery of the counter, and p_1' hits a point E on the surface of the counter 1, the distance of E from the center of the counter surface being a. k, p_1', and p_2' should be on the same plane by the conservation of momentum. The point A on the surface of the counter 2 is obtained by extending the line EO. φ is the angle between AB and C_2A, C_2 being the center of the surface of the counter 2. The angle $\psi(\omega,a,\varphi)$ is a function of ω, a, and φ. Using energy-momentum conservation one can show that

$$\cos\psi\approx 1-\frac{r^2}{2D^2}\frac{E^2}{\omega^2}\left[\left(1-\frac{a^2}{r^2}\sin^2\varphi\right)^{\frac{1}{2}}-\frac{a}{r}\cos\varphi\right]^2. \quad (28)$$

Finally we average over a by assuming that electrons hitting the surface of counter 1 are uniformly distributed. The expression (27) can then be written as

$$\int \frac{d^3p_1'}{E_1'}\int \frac{d^3p_2'}{E_2'}\int \frac{d^3k}{2\omega}\delta(p_1'+p_2'+k-p_1-p_2)$$
$$=\frac{E_1'}{2}d\Omega_1'\int_{\Delta E}^{E}\omega d\omega\int_0^{2\pi}d\varphi\int_0^{r}\frac{2a}{r^2}da$$
$$\times\int_0^{\psi}\frac{\sin\tau d\tau}{s-\omega(1-\cos\tau)}, \quad (29)$$

where τ is the angle between k and p_1'. The term $\omega(1-\cos\tau)$ can be neglected, since when ω is large $(1-\cos\tau)$ is small and vice versa, due to Eq. (28).

From Eq. (29) we can determine what kind of terms in the integrand of Eq. (21) contributes to the logarithmic terms after the integration. Consider $M_b^\dagger M_b$ using Eq. (25). Terms whose denominators are independent of k can be neglected. The term $E_1'=E-\omega$ in some of the denominators does not give any additional logarithmic terms, since there are always equal or more powers of p_1' or E_1' in the numerators. Only those terms with denominators $(p_1'k)$, $(p_1'k)^2$, or ω^2 give logarithmic contributions; among them many are of order $O(m^2/q^2)$ and can be neglected. Hence we can write

$$\sum_{\text{spin}} M_b^\dagger M_b=\frac{e^6}{(2\pi)^7}\frac{1}{2\omega E_1E_2E_1'E_2'}\frac{s^4+q'^4}{q^4}$$
$$\times\left\{\frac{-m^2}{2(p_1'\cdot k)^2}+\frac{E}{\omega(p_1'\cdot k)}\right\}\frac{E_1'}{E}. \quad (30)$$

Similarly

$$\sum_{\text{spin}}\tilde{M}_b^\dagger M_6$$
$$=M_b^\dagger\tilde{M}_b=\frac{-e^6}{(2\pi)^7 2\omega E_1E_2E_1'E_2'}\frac{s^4}{q^2q'^2}$$
$$\times\left\{\frac{-m^2}{2(p_1'\cdot k)^2}+\frac{E}{\omega(p_1'\cdot k)}\right.$$
$$\left.+\frac{E^2}{\omega^2}\left[\frac{s^2}{q^2q'^2}-\frac{E}{E_1'}\frac{q'^4+q^4}{s^2q^2q'^2}+\frac{E^2}{E_1'^2}\frac{2}{s^2}\right]\right\}\frac{E_1'}{E} \quad (31)$$

$$\sum_{\text{spin}}\tilde{M}_b^\dagger\tilde{M}_b$$
$$=\frac{e^6}{(2\pi)^7 2\omega E_1E_2E_1'E_2'}\frac{s^4+q^4}{q'^4}$$
$$\times\left\{\frac{-m^2}{2(p_1'\cdot k)^2}+\frac{E}{\omega(p_1'\cdot k)}\right\}\frac{E_1'}{E}. \quad (32)$$

It can be shown that the terms with a denominator ω^2 in Eq. (31) are much smaller than other terms after the integration, hence they can be neglected. Thus we have

$$\sum_{\text{spin}}(M_b^\dagger M_b-\tilde{M}_b^\dagger M_b-M_b^\dagger\tilde{M}_b+\tilde{M}_b^\dagger\tilde{M}_b)$$
$$=\frac{e_b}{(2\pi)^7 2\omega E_1E_2E_1'E_2'}\left[\frac{s^4+q'^4}{q^4}+\frac{2s^4}{q^2q'^2}+\frac{s^4+q^4}{q'^4}\right]$$
$$\times\left\{\frac{-m^2}{2(p_1'\cdot k)^2}+\frac{E}{\omega(p_1'\cdot k)}\right\}\frac{E_1'}{E}. \quad (33)$$

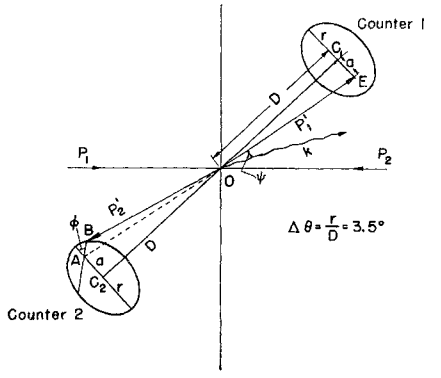

FIG. 5. Geometry used for the calculation of the hard real photon contribution to the cross section for the colliding-beam experiment (Exp. I).

Substituting Eqs. (29) and (33) in Eq. (21) and multiplying by 2 to take into account the emission of a photon by p_2', we obtain the cross section for the emission of hard photons,

$$d\sigma^{\mathrm{I}}{}_{\mathrm{hard}}=d\sigma^{\mathrm{I}}{}_{\mathrm{M\o ller}}\frac{2\alpha}{\pi}\int_{\Delta E}^{E}\frac{d\omega}{\omega}\int_0^{2\pi}d\varphi\int_0^{r}\frac{2a}{r^2}da\int_{\cos\psi}^{1}dx \times\left\{\frac{-m^2}{4E^2(1-\beta_1'x)^2}+\frac{(E-\omega)}{2E(1-\beta_1'x)}\right\}, \quad (34)$$

where $\cos\psi$ is given by Eq. (28) and $\beta_1'=p_1'/E_1'$. After the integration, neglecting the nonlogarithmic terms, we obtain

$$d\sigma^{\mathrm{I}}{}_{\mathrm{hard}}=d\sigma^{\mathrm{I}}{}_{\mathrm{M\o ller}}\frac{2\alpha}{\pi}\left\{\left[\ln\left(\frac{s^2}{m^2}\right)-\ln\left(\frac{16E^2}{(\Delta E)^2\sin^2\theta}\right)\right] \times\left[\ln\left(\frac{E}{\Delta E}\right)-1\right]-2\ln\left(\frac{E}{\Delta E}\right)+\ln^2\left(\frac{E}{\Delta E}\right)\right\} \quad (35)$$

where $\Delta E=2E\Delta\theta/(\sin\theta+\Delta\theta)$. From Eqs. (24) and (35) we can obtain the cross section $d\sigma^{\mathrm{I}}$ for Exp. I. Let

$$d\sigma^{\mathrm{I}}=(d\sigma^{\mathrm{I}}{}_{\mathrm{elastic}}+d\sigma^{\mathrm{I}}{}_{\mathrm{soft}})+d\sigma^{\mathrm{I}}{}_{\mathrm{hard}} \equiv d\sigma^{\mathrm{I}}{}_{\mathrm{M\o ller}}[1+\delta_{\mathrm{soft}}(\theta)+\delta_{\mathrm{hard}}(\theta)],$$

where δ_{soft} and δ_{hard} are radiative corrections to the Møller scattering from $d\sigma^{\mathrm{I}}{}_{\mathrm{elastic}}+d\sigma^{\mathrm{I}}{}_{\mathrm{soft}}$ and $d\sigma^{\mathrm{I}}{}_{\mathrm{hard}}$, respectively. Assuming $E=500$ Mev and $\Delta\theta=3.5°$, we have

$$\delta^{\mathrm{I}}(90°)=\delta^{\mathrm{I}}{}_{\mathrm{soft}}(90°)+\delta^{\mathrm{I}}{}_{\mathrm{hard}}(90°) =(-13.8+4.3)\times10^{-2}=-9.5\times10^{-2},$$

$$\delta^{\mathrm{I}}(35°)=\delta^{\mathrm{I}}{}_{\mathrm{soft}}(35°)+\delta^{\mathrm{I}}{}_{\mathrm{hard}}(35°) =(-8.2+2.2)\times10^{-2}=-6.0\times10^{-2}.$$

The error is estimated to be less than 2% of the cross section which arises from nonlogarithmic terms which we have neglected in the calculation of inelastic and two-photon exchange diagrams.

The fact that the angular dependence of the radiative corrections is rather small is very important experimentally. It shows that the effect due to the radiative corrections does not mar significantly the measurement of the effect due to the possible finite size of the electron which the experiment was originally designed to investigate.

IV. EFFECTS DUE TO POSSIBLE BREAKDOWN OF QUANTUM ELECTRODYNAMICS

The effects on various physical processes due to the possible breakdown of QED have been discussed extensively by many authors.[1,13] We discuss here how this breakdown in QED may manifest itself in Exp. I. There are two possible sources which may alter the Møller formula at high energies. First, an electron may not be a point particle, but may have some kind of charge distribution. In this case we may associate with each vertex a form factor $F_e(q^2)$ analogous to the charge form factor $F_p{}^1(q^2)$ used in the analysis of electron-proton scattering.[13] [The magnetic form factor used in electron-proton scattering can be neglected in our case, since we have shown that the contribution to the cross section from the anomalous magnetic moment of the electron is of order $\sigma^{\mathrm{I}}{}_{\mathrm{M\o ller}}(\alpha m^2/\pi q^2)\ln(-q^2/m^2)$.] Second, the Coulomb law may not hold at small distances. This is equivalent to changing the photon propagator, $1/q^2\rightarrow C(q^2)/q^2$. Since each photon propagator is connected with two vertices we may use the substitution $1/q^2\rightarrow C(q^2)F_e{}^2(q^2)/q^2$. We may assume $C(q^2)$ to be in the form of the Feynman regulator for the photon propagator,[1] $C(q^2)=(1-q^2/\Lambda^2)^{-1}$ and[13] $F_e(q^2)=(1-\langle r_e{}^2\rangle q^2/6)^{-1}$. Λ^{-1} represents a measure of the distance at which the Coulomb law breaks down and $\langle r_e{}^2\rangle$ is the relativistic generalization of the mean square radius of the static charge distribution of the electron. We notice that it is impossible to determine $C(q^2)$ and $F_e(q^2)$ separately by Exp. I. In fact, no experiment involving only electrons and photons can do this, since they always appear in the form $C(q^2)\times F_e{}^2(q^2)$. Thus we choose a simpler form and define

$$G(q^2)\equiv C(q^2)F_e{}^2(q^2)\equiv\frac{1}{1-q^2/K^2}, \quad (36)$$

where

$$1/K^2\approx\langle r_e{}^2\rangle/3+1/\Lambda^2. \quad (37)$$

Replacing $1/q^2$ by $G(q^2)/q^2$, Eq. (3) can be written as

$$d\sigma^{\mathrm{I}}{}_{\mathrm{M\o ller}}=\frac{r_0{}^2}{8}\frac{E^2}{m^2}d\Omega_1'\left[\frac{s^4+q'^4}{q^4}G^2(q^2) +\frac{2s^4}{q^2q'^2}G(q^2)G(q'^2)+\frac{s^4+q^4}{q'^4}G^2(q'^2)\right]. \quad (38)$$

Table I shows the effect of $G(q^2)$ on the counting rate per unit solid angle at 90° and 35° for various values of K^{-1}. The counting rates are arbitrarily normalized; they represent the numerical values obtained from the terms inside the bracket of Eq. (38).

$K^{-1}=0$ or $G(q^2)=1$ represents the case of no breakdown in quantum electrodynamics. $K^{-1}=0.05$ fermi represents the smallest distance which Exp. I can

TABLE I. The effect of $G(q^2)$ on the relative differential cross sections at 90° and 35° for the clashing-beam experiment with $E=500$ Mev.

K^{-1}, fermi	$\theta=90°$	$\theta=35°$
0	18	248.8
0.33	18/5.73	248.8/1.67
0.05	18/1.075	248.8/1.017

[13] D. R. Yennie, M. M. Levy, and D. G. Ravenhall, Revs. Modern Phys. **29**, 144 (1957).

presumably probe. From the electron-proton scattering we have

$$F_e(q^2)C(q^2)F_p{}^1(q^2) = F_p{}^1(q^2)_{\rm obs} = \frac{1}{1-(0.8\text{ fermi})^2q^2/6}. \quad (39)$$

Notice in this case $F_e(q^2)$ and $C(q^2)$ do not appear in the form $C(q^2)F_e{}^2(q^2)$ as in Exp. I. Thus the true proton form factor $F_p{}^1(q^2)$ cannot be obtained from the results of Exp. I and electron-proton scattering. In order to determine $F_p{}^1(q^2)$, one has to know $F_e(q^2)$ and $C(q^2)$ separately and it can be shown easily that it is impossible to design any experiment to do this. If $F_p{}^1(q^2)=C(q^2)=1$, then from Eqs. (36) and (39) one obtains $K^{-1}=0.46$ fermi which is the upper limit on K^{-1} given by electron-proton scattering. Similarly if $F_p{}^1(q^2)=F_e(q^2)=1$, then one obtains $K^{-1}=0.33$ fermi, whose effect on the cross section is shown in Table I. In conclusion, we should mention that Exp. I gives information about $G(q^2)$ for space-like q. The electron-positron clashing beam experiment which is also being planned at Stanford will give information about $G(q^2)$ for time-like q. (See Sec. VI.) Similar to the modification of the photon propagator when $|q^2|\gg 0$, one might expect modification of the electron propagator $(\not{p}-m)^{-1}$ when p is far from its mass shell, i.e., $|p^2|\gg m^2$. To test the modification of the electron propagator one has to perform experiments such as Compton scattering, pair production by electrons[14] or photons[7] in the proton field, or $e^+ + e^- \to 2\gamma$.

V. INELASTIC SCATTERING FOR EXPERIMENT II

It is most convenient to calculate this cross section in the center-of-mass system.[15] In order to do this, we have to transform all the experimental conditions for Exp. II into the conditions in the center-of-mass system. All the quantities in the laboratory system are denoted by a bar on top of each quantity. The geometry for Exp. II is shown in Fig. 6. The entrance slit S_1 selects those final electrons scattered into the solid angle subtended by it. The final slit S_2 selects those electrons whose energy is within the range $\bar{E}_1{}'_{\min}<\bar{E}_1{}'<\bar{E}_1{}'_{\max}$. This energy range is very small compared with $\bar{E}_1{}'$ (about 0.25%), thus we may assume $\bar{E}_1{}'$ to have a definite value. For the elastic scattering, there is a one-to-one correspondence between $\bar{E}_1{}'$ and the scattering angle $\bar{\theta}$. Thus we define this angle as $\bar{\theta}_{\rm elastic}$. $\bar{\theta}_{\max}$ and $\bar{\theta}_{\min}$ are the maximum and minimum angles defined by the entrance slit S_1 as shown in Fig. 6. It will be shown later that no electrons with scattering angle greater than $\bar{\theta}_{\rm elastic}$ (strictly speaking the angle which corresponds to $\bar{E}_1{}'_{\min}$ in the elastic scattering) can go into S_2, and the radiative correction depends upon the quantity $\Delta\bar{\theta}=\bar{\theta}_{\rm elastic}-\bar{\theta}_{\min}$ rather than the energy resolution of the spectrometer $\Delta\bar{E}_1{}'=\bar{E}_1{}'_{\max}-\bar{E}_1{}'_{\min}$ if $\Delta\bar{E}_1{}'$ is much smaller than the energy difference between two elastically scattered electrons at angles $\bar{\theta}_{\min}$ and $\bar{\theta}_{\rm elastic}$.

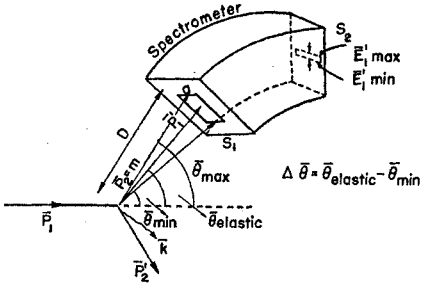

FIG. 6. Geometry for Exp. II.

Now let us transform all of our experimental conditions into those in the center-of-mass system. The incident energy $E_1=E_2$ can be obtained from the invariant $p_1\cdot p_2$:

$$p_1\cdot p_2 = m\bar{E}_1 = E_1{}^2+P^2 = 2E_1{}^2-m^2;$$

thus

$$E_1 \approx (m\bar{E}_1/2)^{\frac{1}{2}}. \quad (40)$$

In the laboratory system we detect those electrons which are scattered with angles between $\bar{\theta}_{\max}$ and $\bar{\theta}_{\min}$ and have energies between $\bar{E}_1{}'_{\max}$ and $\bar{E}_1{}'_{\min}$. The angle $\bar{\theta}$ and the energy $\bar{E}_1{}'$ can be expressed in terms of the center-of-mass quantities by choosing suitable invariant quantities. For example,

$$\frac{m^2(p_1\cdot p_1')}{(p_1\cdot p_2)(p_1'\cdot p_2)} = \frac{m^2}{2E_1{}^2}\tan^2(\theta/2) = (1-\cos\bar{\theta}) \approx \bar{\theta}^2/2, \quad (41)$$

$$p_1'\cdot p_2/m = \bar{E}_1{}' = (E_1'E_1/m)(1+\cos\theta),$$

or

$$E_1' = m\bar{E}_1'/E_1(1-\cos\theta). \quad (42)$$

From Eq. (41) we can determine the maximum and minimum angles $\theta_{\max}$ and $\theta_{\min}$ in the center-of-mass system; we obtain

$$\tan(\theta_{\max}/2) = (E_1/m)\bar{\theta}_{\max}, \quad (43)$$

$$\tan(\theta_{\min}/2) = (E_1/m)\bar{\theta}_{\min}. \quad (44)$$

From Eq. (42) we can determine the maximum and minimum energies of the detected electrons in the center-of-mass system:

$$E_1'{}_{\max} = m\bar{E}_1'{}_{\max}/E_1(1+\cos\theta), \quad (45)$$

$$E_1'{}_{\min} = m\bar{E}_1'{}_{\min}/E_1(1+\cos\theta). \quad (46)$$

From energy-momentum conservation, we have

$$E_1' \leqslant E_1. \quad (47)$$

We plot the boundary obtained by Eqs. (43) to (47) on a (θ,E_1') plane (see Fig. 7). The electrons which are detected must be in the shaded area as shown in Fig. 7.

[14] J. D. Bjorken and S. D. Drell, Phys. Rev. **114**, 1368 (1959).
[15] The author is grateful to Dr. J. D. Bjorken for several suggestions on this section. (See the discussion in Sec. VII D.)

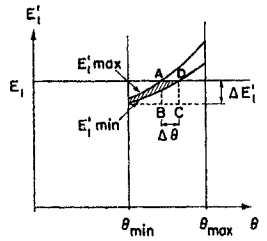

FIG. 7. Geometry for Exp. II expressed in terms of the quantities in the center-of-mass system.

Thus we have accomplished transforming the experimental conditions for Exp. II into those in the center-of-mass system. Since the majority of the electrons have energies very close to E_1, we may approximate the number of electrons going into this shaded area by the number of electrons going into the area $ABCD$. The width a of the entrance slit S_1 in Fig. 6 is not changed by the coordinate transformation. Let us denote the lengths of AB and BC by $\Delta E_1'$ and $\Delta\theta$, respectively. Then our consideration shows that Exp. II is equivalent to an experiment in the center-of-mass system with a single counter which has an energy resolution $\Delta E_1'$ and a rectangular entrance slit defined by a and $\Delta\theta$. $\Delta E_1'$ and $\Delta\theta$ can be calculated easily from Eqs. (43) to (47). We obtain

$$\Delta\theta = m\Delta\bar{E}_1'/E_1^2 \sin\theta, \tag{48}$$

$$E_1/\Delta E_1' = [s^2/(-q^2)]\bar{\theta}_{\text{elastic}}/2\Delta\bar{\theta}. \tag{49}$$

Under the condition of Exp. II, $\Delta\theta$ is about 1/400 radian. The maximum energy of photons which can be emitted in the direction of p_1' is $\Delta E_1'$, thus from Eq. (49), the quantity $\Delta E_1'$ which comes into the radiative correction is dependent upon $\Delta\bar{\theta}$ rather than the energy resolution of the spectrometer $\Delta\bar{E}_1'$. This is one of the essential differences between the radiative corrections to $e-e$ scattering and $e-p$ scattering as mentioned in the introduction. Let us denote the maximum energies of photons which can be emitted along p_1, p_2, and p_2' directions by ΔE_1, ΔE_2, and $\Delta E_2'$, respectively. We can calculate ΔE_1, ΔE_2, and $\Delta E_2'$ easily from energy-momentum conservation. The results are

$$\frac{E_1}{\Delta E_1}\approx\frac{q'^2\bar{\theta}_{\text{elastic}}}{q^2 2\Delta\bar{\theta}},\quad \frac{E_1}{\Delta E_2}\approx\frac{\bar{\theta}_{\text{elastic}}}{2\Delta\bar{\theta}},\quad \text{and}\quad \frac{E_1}{\Delta E_2'}=1. \tag{50}$$

Unlike the situation in Exp. I, in this case ΔE_1 and ΔE_2 are independent of $\Delta\theta$. This is because in this case firstly $\Delta\theta$ is very small and secondly we have a single counter instead of two coincident counters as in the case of Exp. I. It is interesting to observe that approximately $\bar{\theta}/2\Delta\bar{\theta}$ in Exp. II plays the role of $E/\Delta E$ in the center-of-mass system except for the photons emitted along the direction of p_2' where the photon can steal almost all the energy from p_2'. Under the experimental condition $\bar{\theta}_{\text{elastic}}\gg 2\Delta\bar{\theta}$, we have ΔE_1, ΔE_2, $\Delta E_1'\ll E_1$.

Let us define

$$\Delta E = (\Delta E_1\Delta E_2\Delta E_1')^{\frac{1}{3}}. \tag{51}$$

We first integrate the photon momentum K from 0 to ΔE assuming an isotropic $K_{\max}=\Delta E$. Denoting this cross section as $d\sigma^{\text{II}}{}_{\text{soft}}$, we have from Eq. (22)

$$d\sigma^{\text{II}}{}_{\text{soft}} = -d\sigma^{\text{II}}{}_{\text{Møller}}\frac{4\alpha}{\pi}\left\{\ln\left(\frac{E_1}{\Delta E}\right)\left[\ln\left(\frac{q^2q'^2}{s^2m^2}\right)-1\right]+\frac{1}{4}\left[4\ln\left(\frac{m}{\lambda}\right)+s^2\mu_2(-s^2)+q^2\mu_2(q^2)+q'^2\mu_2(q'^2)\right]\right\}. \tag{52}$$

This cross section represents approximately the inelastic cross section in which the maximum energies of photons emitted by p_1, p_2, p_1' and p_2' are ΔE_1, ΔE_2, $\Delta E_1'$, and ΔE, respectively. This statement is quite plausible in itself; in fact we have used a much more elaborate method [the coordinate system in which $(k+p_2')_j=0$, where $j=1, 2, 3$] to calculate the same cross section and the results indicate that our statement is true. Since the maximum energy of photons which can be emitted by p_2' is E_1, we must add to Eq. (52) the cross section for the photons emitted by p_2' with energies from ΔE to E_1. We call this the hard photon cross section for Exp. II and denote it by $d\sigma^{\text{II}}{}_{\text{hard}}$. This cross section can be calculated by using Eq. (34) (divide it by 2, since we are considering the photons emitted by p_2' only). The maximum angle ψ between k and p_2' in Eq. (34) is a very complicated function of the magnitude of E_1' and the vector K. In general ψ is smaller for larger K and E_1' and vice versa. Since most photons emitted by p_2' are along p_2' direction and the number of soft photons emitted is usually much greater than that of hard photons, the result is not very much dependent on ψ. Thus we will approximate ψ by $\pi/2$, and obtain

$$d\sigma^{\text{II}}{}_{\text{hard}} = d\sigma^{\text{II}}{}_{\text{Møller}}\frac{2\alpha}{\pi}\int_{\Delta E}^{E_1}\frac{d\omega}{\omega}\int_0^1 dx\times\left[\frac{-m^2}{4E_1^2(1-\beta_2'x)^2}+\frac{(E_1-\omega)}{2E_1(1-\beta_2'x)}\right]$$
$$\approx d\sigma^{\text{II}}{}_{\text{Møller}}\frac{\alpha}{\pi}\left\{\left[\ln\left(\frac{s^2}{2m^2}\right)-1\right]\times\ln\left(\frac{E_1}{\Delta E}\right)-\ln\left(\frac{s^2}{2m^2}\right)\right\}. \tag{53}$$

Here we have used the relation $\beta_2'=p_2'/E_2'$ and $E_2'\approx E_1-\omega$.

From Eqs. (18), (52), and (53) we obtain the cross section $d\sigma^{II}$ for Exp. II:

$$d\sigma^{II}=d\sigma^{II}_{\text{elastic}}+d\sigma^{II}_{\text{soft}}+d\sigma^{II}_{\text{hard}}$$
$$=\frac{r_0^2}{2}\frac{m}{\bar{E}_1^2}\frac{a\Delta\bar{E}_1'}{D\sin\bar{\theta}_{\text{elastic}}}\left\{\left(\frac{s^4+q'^4}{q^4}+\frac{s^4}{q'^2q^2}\right)\times\left[1-\frac{4\alpha}{\pi}\left(\frac{23}{18}-\frac{11}{12}\ln\left(\frac{-q^2}{m^2}\right)\right)\right]+\text{exchange}\right\}$$
$$-d\sigma^{II}_{\text{Møller}}\frac{4\alpha}{\pi}\left\{\ln\left(\frac{E_1}{\Delta E}\right)\left[\ln\left(\frac{q^2q'^2}{s^2m^2}\right)-1\right]-\frac{1}{4}\ln\left(\frac{E_1}{\Delta E}\right)\left[\ln\left(\frac{s^2}{2m^2}\right)-1\right]+\frac{1}{4}\ln\left(\frac{s^2}{2m^2}\right)\right\}. \quad (54)$$

We have neglected the terms $f(x)+f(1-x)$, since they are negligible. For $\theta\gtrsim 90°$, we may write Eq. (54) approximately as

$$d\sigma^{II}=d\sigma^{II}_{\text{Møller}}[1+\delta(\theta)],$$

where

$$\delta(\theta)_{\theta\gtrsim 90°}\approx-\frac{4\alpha}{\pi}\left\{\frac{23}{18}-\frac{11}{12}\ln\left(\frac{-q'^2}{m^2}\right)+\ln\left(\frac{E_1}{\Delta E}\right)\left[\ln\left(\frac{q^2q'^2}{s^2m^2}\right)-1\right]-\frac{1}{4}\ln\left(\frac{E_1}{\Delta E}\right)\times\left[\ln\left(\frac{s^2}{2m^2}\right)-1\right]+\frac{1}{4}\ln\left(\frac{s^2}{2m^2}\right)\right\}. \quad (55)$$

$\delta(\theta)$ is the radiative correction for Exp. II. It should be noticed that there is no term like $\alpha\ln^2(-q^2/m^2)$ in our expression for $\delta(\theta)$. The quantities ΔE in Eq. (55) can be expressed in terms of the laboratory quantity $\Delta\bar{\theta}$ by using Eqs. (49), (50), and (51). The numerical values for $\delta(\theta)$ for various values of θ and $\bar{\theta}_{\text{elastic}}/2\Delta\bar{\theta}$ are given in Table II. The error in our calculation is estimated to be less than 2% of the cross section, which arises from the nonlogarithmic terms which we have neglected in the calculation of two-photon exchange diagrams and the hard real photon contribution. The experimental values given in Table II are preliminary results supplied by Dally.

TABLE II. The radiative corrections for Exp. II.

$\bar{E}_1$ Mev	θ	$\bar{\theta}_{\text{elastic}}/2\Delta\bar{\theta}$	Calculated $\delta(\theta)$, %	Experimental $\delta(\theta)$, %
502	90°	9.7	−5.5±2	−3.6±2.4
502	107°	10.3	−4.9±2	−3.5±2.9
502	120°	13.2	−4.9±2	−6.0±2.4

VI. ELECTRON-POSITRON SCATTERING

The workers associated with Exp. I are also planning to do the electron-positron clashing beam experiment with the energy range between 100 and 500 Mev (possibly higher). In this energy range the following interactions are possible[16]:

(a) $e^++e^-\to e^++e^-$,
(b) $e^++e^-\to\mu^++\mu^-$,
(c) $e^++e^-\to\pi^++\pi^-$,
(d) $e^++e^-\to\pi^++\pi^-+\pi^0$,
(e) $e^++e^-\to K^++K^-$,
(f) $e^++e^-\to K^0+\bar{K}^0$.

Interactions (b) through (f) involve only a pure time-like photon as an intermediate state. Thus the final states should have total energy $2E$, total momentum zero, total charge zero, total angular momentum one, negative charge parity and zero strangeness. Two- and three-π^0 states are prohibited because they have even charge parity. For final states involving only two spinless particles, the orbital angular momentum must be one, i.e., in P state [see Eq. (58)]. Incidentally, the two-π^0 state is prohibited also from statistics since two identical bosons cannot be in the P state. Energetically more pions than three can be produced, but we will not treat them here because we do not know how to handle the problem. We shall simply point out that, from the conditions that the system must be neutral and odd under charge conjugation, the number of different kinds of pions produced must satisfy $(2n+1)\times(\pi^++\pi^-)+l\pi^0$, where n and l are arbitrary integers.[17] In the following, we calculate the cross sections for the processes from (a) through (f) in order to facilitate the experimental design and further theoretical investigations.

(a) The elastic and the soft real photon parts of the cross section to order α^3 of the process $e^++e^-\to e^++e^-$ can be obtained from the result of our present calculation for Exp. I by the well-known substitution law $p_1\to-p_+'$ and $p_1'\to-p_+$, where p_+ and p_+' are the four-momenta of incident and outgoing positrons, respectively. These substitutions are equivalent to the substitution $q'^2\leftrightarrow s^2$. For example, the Bhabha cross section with form factors can be written as

$$\frac{d\sigma}{d\Omega(e^+)}=\frac{r_0^2}{8}\frac{m^2}{E^2}\left[\frac{s^4+q'^4}{q^4}|G(q^2)|^2+\frac{2q'^4}{q^2s^2}|G(q^2)G(s^2)|+\frac{q'^4+q^4}{s^4}|G(s^2)|^2\right], \quad (56)$$

[16] *Note added in proof.*—This list is not complete. The most obvious omissions are the processes $e^++e^-\to 2\gamma$ and $e^++e^-\to\gamma+\pi^0$. The cross section for the first process can be found in reference 10. The second process is being studied and the result will be published later.

[17] S. D. Drell and F. Zachariasen, *Electromagnetic Structure of Nucleons* (Oxford University Press, Oxford, 1960, to be published).

where $s^2=(p_+ + p_-)^2$, $q^2=(p_+ - p_+')^2$, $q'^2=(p_+ - p_-')^2$, and $G(q^2)$ is defined in Sec. IV. This experiment gives information about the form factor with time-like momentum transfer $G(s^2)$ in addition to $G(q^2)$. The radiative corrections due to hard real photons cannot be calculated unless the experimental conditions are specified, as we have repeatedly emphasized in this paper.

(b) The cross section for the process $e^+ + e^- \to \mu^+ + \mu^-$ to order α^2 with form factors can be calculated easily and we have (neglecting the magnetic form factor of muons)

$$\frac{d\sigma}{d\Omega(\mu^+)}=\frac{r_0^2}{8}\frac{m^2}{E^2}\frac{(E^2-m_\mu^2)^{\frac{1}{2}}}{E}\left[\frac{1+\cos^2\theta}{2}+\frac{m_\mu^2}{2E^2}\sin^2\theta\right]\times|F_e(s^2)C(s^2)F_\mu(s^2)|^2, \quad (57)$$

where m_μ is the muon rest mass and $F_\mu(s^2)$ is the muon (charge) form factor normalized such that $F_\mu(0)=1$. This experiment gives information about $F_\mu(s^2)$ for time-like momentum transfer. The radiative corrections to this process have not been calculated.

(c) The first-order cross section for the process $e^+ + e^- \to \pi^+ + \pi^-$, with form factors, can be calculated easily, and we have[18]

$$\frac{d\sigma}{d\Omega(\pi^+)}=r_0^2\frac{m^2}{32E^2}\frac{(E^2-\mu^2)^{\frac{3}{2}}\sin^2\theta}{E^3}\times|F_e(s^2)C(s^2)F_\pi(s^2)|^2, \quad (58)$$

where μ is the pion rest mass and $F_\pi(s^2)$ is the pion form factor with time-like momentum transfer normalized such that $F_\pi(0)=1$ (see the Appendix). It will be interesting to see if the pion form factor obtained from this experiment agrees with the ones advanced by various authors[19,20] in order to explain the isotopic vector parts of the nucleon form factors.

(d) The discussion for the process $e^+ + e^- \to \pi^+ + \pi^- + \pi^0$ will be more or less just a conjecture due to the uncertainty even in the form of the coupling $(\gamma,3\pi)$. Assuming the interaction between the photon and the three-pion state to be of the form[21]

$$H_{\rm int}=ie\left(\frac{\lambda}{\mu^3}\right)\epsilon_{\mu\nu\alpha\beta}A_\mu\frac{\partial\phi_+}{\partial x_\nu}\frac{\partial\phi_-}{\partial x_\alpha}\frac{\partial\phi_0}{\partial x_\beta}, \quad (59)$$

where $\epsilon_{\mu\nu\alpha\beta}$ is the Levi-Civitá symbol in four-dimensional space and λ the coupling constant, we obtain[22]

$$\langle 0|j_\mu(0)|\pi^+\pi^-\pi^0\rangle=-i(8\omega_+\omega_-\omega_0)^{-\frac{1}{2}}\epsilon_{\mu\nu\alpha\beta}p_\nu^+ p_\alpha^- p_\beta^0\frac{e\lambda}{\mu^3}. \quad (60)$$

In the center-of-mass system we have

$$\epsilon_{\mu\nu\alpha\beta}p_\nu^+ p_\alpha^- p_\beta^0=2E(\mathbf{P}^+\times\mathbf{P}^-)_\mu. \quad (61)$$

Thus the cross section can be written as

$$d\sigma=\frac{\alpha^2}{32\pi^3}\frac{\lambda^2}{\mu^6}\frac{1}{s^2}(\mathbf{P}^+\times\mathbf{P}^-)^2\sin^2\theta\times\int P^+ d\omega^+ d\Omega^+\int P^- d\omega^- d\Omega^-\times|F_e(s^2)C(s^2)|^2\delta((p^+ + p^- - s)^2-\mu^2), \quad (62)$$

where θ is the angle between the incident electron and $(\mathbf{P}^+\times\mathbf{P}^-)$. Assuming the experimental conditions to be such that $d\omega^+$, $d\Omega^+$, and $d\Omega^-$ are fixed, we have[18]

$$\frac{d^3\sigma}{d\omega^+ d\Omega^+ d\Omega^-}=r_0^2\frac{m^2}{32E^2}\frac{1}{(2\pi)^3}\frac{1}{\mu^6}(\mathbf{P}_+\times\mathbf{P}_-)^2\sin^2\theta\times\frac{P_+P_-|F_e(s^2)C(s^2)F_{3\pi}(s^2,\omega_+,\omega_-)|^2}{(2E-\omega_+ + P_+\omega_-\cos\varphi/P_-)}, \quad (63)$$

where φ is the angle between the momenta of two charged pions p^+ and p^-. We have replaced λ by $F_{3\pi}(s^2,\omega_+,\omega_-)$ to take into account the possible dependence of λ^2 on s^2, ω_+, and ω_- in more generalized types of interactions than Eq. (59). From Eq. (63) it is obvious that the cross section is maximum when $\theta=\pi/2$, i.e., all incident and final particles are on the same plane, and the term $(\mathbf{P}_+\times\mathbf{P}_-)^2$ becomes maximum, i.e., the area formed by the momenta of the three final particles is maximum. The information on $F_{3\pi}(s^2,\omega_+,\omega_-)$ obtained from this experiment is useful for accounting for the isotopic scalar part of the nucleon form factors.[17,22,23]

(e), (f). Assuming K mesons to be spinless particles, then the cross sections for producing $K^+ + K^-$ and $K_0 + \bar{K}_0$ can be expressed by Eq. (58) with the pion rest mass μ replaced by the K particle rest mass $m_K \approx 494$ Mev, and the pion form factor $F_\pi(s^2)$ replaced by $F_{K^\pm}(s^2)$ and $F_{K^0}(s^2)$, respectively. $F_{K^\pm}(s^2)$ and $F_{K^0}(s^2)$ are normalized such that $F_{K^\pm}(0)=1$ and $F_{K^0}(0)=0$. The cross sections for these two processes are very small because $E\sim m_K$ and thus the phase space available for the interaction is very small as can be seen from Eq. (58). However, the workers associated with Exp. I hope to be able to raise the energy E up to about 650 Mev so that detailed investigations of these two processes may be feasible.[24]

VII. DISCUSSION

A. We have shown that the radiative corrections to Exp. I are rather small, namely -9.5 ± 2 and $-6.0\pm2\%$

[18] Slightly different but similar results have been obtained by N. Cabibbo and R. Gatto, Phys. Rev. Letters 4, 313 (1960).
[19] W. Frazer and J. Fulco, Phys. Rev. **117**, 1609 (1960).
[20] M. Baker and F. Zachariasen, Phys. Rev. **118**, 1659 (1960).
[21] B. Bosco and V. De Alfaro, Phys. Rev. **115**, 215 (1959).
[22] P. Federbush, M. L. Goldberger, and S. B. Treiman, Phys. Rev. **112**, 642 (1958).
[23] G. F. Chew, R. Karplus, S. Gasiorowicz, and F. Zachariasen, Phys. Rev. **110**, 265 (1958).
[24] W. K. H. Panofsky and B. Richter (private communication).

at 90° and 35°, respectively. Since only angular distributions (not the absolute cross sections) will be measured experimentally, the angular dependence of the radiative corrections is the only thing which is important here. The radiative corrections depend upon q^2 and ΔE [see Eqs. (24) and (35), notice ΔE depends upon θ], both of which tend to make the radiative corrections larger at 90° than 35°. The two percent error shown is from the nonlogarithmic terms which we have neglected in the evaluation of two-photon exchange diagrams and the hard real photon cross sections, which we do not expect to be very angular dependent. Thus the error in the angular dependence of the radiative corrections is probably less than 1% of the cross section. The angular dependence of the contributions from vacuum polarizations due to heavier particles in the closed loop as discussed in the Appendix is for all practical purposes negligible (+0.3% corrections at most).

B. Two-photon exchange diagrams are shown to have only negligible contributions to the cross section except the infrared terms which cancel out eventually with the corresponding terms in the inelastic cross section. It is interesting to see if this is still true for the radiative corrections for processes such as

$$e^+ + e^- \to \mu^+ + \mu^-,$$
$$\mu^- + e^- \to \mu^- + e^-,$$
$$e^- + p \to e^- + p.$$

C. One of the most important results which we have obtained in this paper is that there is no term like $\alpha \ln^2(-q^2/m^2)$ (compared with unity) in the radiative corrections for high-energy $e-e$ scattering, unless one assumes some unrealistic experimental conditions such as $K_{\max}$ is isotropic and $\ll m$. As the energy and the accuracy of the experiments involving charged particles increase, detailed calculations of the radiative corrections such as we have made in this paper may become more important in the future. For example, the radiative corrections to processes mentioned in Sec. VI will eventually be carried out using the method similar to the present calculation.

D. In the calculation of the inelastic cross sections for Exp. II, we used the center-of-mass system. This is by no means just because we wanted to use the result of the calculation of Exp. I. In fact we tried to calculate the cross sections in two other coordinate systems, namely, the laboratory system and the barycentric system of the two undetected final particles (the coordinate system in which $\mathbf{p}_2'+\mathbf{k}=0$). Both of these coordinate systems are found to be impractical for dealing with high-energy processes involving hard photons. Using the laboratory system, we found that the calculation becomes impossibly complicated unless one assumes $K_{\max}$ is isotropic and $\ll m$. (Incidentally, we confirmed Redhead[3] and Polovin's[4] result in the high-energy limit and under the assumption that $K_{\max}$ is isotropic and $\ll m$ in the laboratory system.) The coordinate system in which $\mathbf{k}+\mathbf{p}_2'=0$ was tried because in this coordinate system the photon angular integration becomes extremely simple. However, this coordinate system was also found to be inconvenient because in this coordinate system it is very difficult to determine what terms in the matrix elements (there are more than one thousand terms) can be neglected.

VIII. ACKNOWLEDGMENTS

The author wishes to thank Professor S. D. Drell for numerous suggestions and criticisms on the manuscript, and Professor D. R. Yennie, Dr. J. D. Bjorken, Dr. S. C. Frautschi, and Dr. H. Suura for useful discussions. He is also indebted to Professor M. Baker and Professor F. Zachariasen for suggestions on the Appendix. He is grateful to Dr. Edgar B. Dally for explaining to him the details of his experiment and for the permission to quote the results before his publication. Finally, the author must express his indebtedness to workers associated with the colliding-beam experiments, especially Professors W. K. H. Panofsky and B. Richter, for discussions of many experimental details.

APPENDIX: VACUUM POLARIZATIONS

The closed loop in the vacuum polarization diagram M_4 is assumed to be an electron pair in our calculation. But in reality it can be a pair of any other particles or even three or more particle states of various particles; for example a muon pair, a pion pair, a nucleon pair or three-pion state $\pi^+ + \pi^- + \pi^0$. It is interesting to investigate how these various kinds of intermediate states in the photon propagator affect the cross section of $e-e$ scattering. The matrix element M_4 for a pair of structureless fermions in the closed loop can be written as[9,25]

$$M_4(\text{fermions}) = M_1 \frac{\alpha}{\pi}\left[\frac{-5}{9}+\frac{4}{3x^2}+\frac{1}{3}\left(1+\frac{4}{x^2}\right)^{\frac{1}{2}} \times\left(1-\frac{2}{x^2}\right)\ln\left(\frac{(1+4/x^2)^{\frac{1}{2}}+1}{(1+4/x^2)^{\frac{1}{2}}-1}\right)\right], \quad \text{(A1)}$$

where $x^2=-q^2/M^2$ and M is the rest mass of the particle in the closed loop. Similarly the matrix element M_4 for a pair of structureless bosons in the closed loop can be written as[9] [see also Eq. (A8)]

$$M_4(\text{bosons}) = M_1 \frac{\alpha}{\pi}\left[\frac{-4}{9}-\frac{4}{3x^2}+\frac{1}{6}\left(1+\frac{4}{x^2}\right)^{\frac{1}{2}} \times\ln\left(\frac{(1+4/x^2)^{\frac{1}{2}}+1}{(1+4/x^2)^{\frac{1}{2}}-1}\right)\right]. \quad \text{(A2)}$$

Assuming electrons, muons, and protons to be pure

[25] R. N. Euwema and J. A. Wheeler, Phys. Rev. 103, 803 (1956).

Dirac particles, we can calculate the contributions to the cross section for Exp. I easily by using Eqs. (A1) and (1). At 90° the contributions to the cross section are about +2, +0.35, and +0.02%, respectively, for electron, muon and proton pairs in the closed loop. Similarly for a structureless pion pair the contribution to the cross section for Exp. I at 90° is [from Eqs. (A2) and (1)] +0.089%. Thus the contributions to the cross section are negligible except for the electron pair which we have already considered in the text.

Next let us consider the effect of the form factors of the particles in the closed loop. The form factors of various particles are still to be determined by the experiments discussed in Sec. VI. However there exist several conjectures[19,20] about the pion form factor $F_\pi(q^2)$ so we discuss this case as an example.[26] According to references 19 and 20, $F_\pi(q^2)$ is related to the $\pi-\pi$ interaction which has a resonance in the $J=1$, $I=1$ state of two pions. Thus we want to investigate how this $\pi-\pi$ interaction may enhance the cross section for e^-e^- scattering. The pion form factor $F_\pi(q^2)$ is defined as a vertex function consisting of one virtual photon whose four-momentum is q (which may be either space-like or time-like) and two "real" pions. It is normalized such that $F_\pi(0)=1$. This simply means that we replace e associated with the above defined vertex in the perturbation theory by $eF_\pi(q^2)$. Let us consider photon propagators with two-pion intermediate states as shown in Fig. 8(a) and 8(b), where the blobs represent the effects due to the pion structure. We may not replace e by $eF_\pi(q^2)$ in Fig. 8(a) [$eF_\pi(s^2)$ in Fig. 8(b)] because the pions in the loop are not necessarily real. [In fact they can never be real for space-like photons such as are shown in Fig. 8(a).] For a time-like photon as shown in Fig. 8(b), the two-pion intermediate states may become real when $s^2>4\mu^2$, and the real intermediate states contribute to the absorptive part of the matrix element. Thus one may replace e by $eF_\pi(s^2)$ in the absorptive part of the matrix element obtained by the perturbation method. We then use this modified absorptive part of the matrix element to obtain the modified matrix element by the dispersion relations. From perturbation theory, the matrix element for the photon propagator with two-pion intermediate states

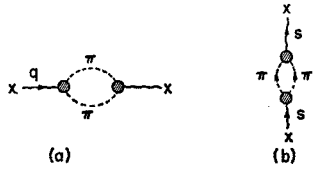

FIG. 8. (a) Space-like photon propagator with two-pion intermediate states; (b) time-like propagator with two-pion intermediate states.

[26] After this work was completed, an article by L. M. Brown and F. Calogero appeared in Phys. Rev. Letters 4, 315 (1960), which treated the same problem. We include our treatment here for completeness. They suggest that this effect may be used for the determination of $F_\pi(q^2)$. However, our emphasis here is to prove that this effect is negligible compared with the error in the calculation of the radiative corrections which is about 2%.

FIG. 9. Electron-electron scattering with two-pion intermediate states in the photon propagator.

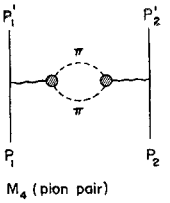

may be written as

$$\frac{-1}{2}D_F'(q^2)g_{\mu\nu}=\frac{ig_{\mu\nu}}{(2\pi)^4}\frac{\alpha}{\pi}f(q^2), \tag{A3}$$

where

$$f(q^2)=-\frac{1}{q^2}\left[\frac{4}{9}-\frac{4\mu^2}{3q^2}-\frac{1}{6}\left(1-\frac{4\mu^2}{q^2}\right)^{\frac{3}{2}}\times\ln\left(\frac{(1-4\mu^2/q^2)^{\frac{1}{2}}+1}{(1-4\mu^2/q^2)^{\frac{1}{2}}-1}\right)\right]. \tag{A4}$$

Here q may be either time-like or space-like. From the analytic properties of $f(z)$, which is the analytic continuation of $f(q^2)$, we can verify easily the dispersion relation

$$f(q^2)=\frac{1}{\pi}\int_{4\mu^2}^{\infty}\frac{\mathrm{Im}f(s^2)ds^2}{s^2-q^2-i\epsilon}, \tag{A5}$$

where $\mathrm{Im}f(s^2)$ can be obtained easily from (A4). $\mathrm{Im}f(s^2)$ represents the absorptive process, and the pion form factor $F_\pi(s^2)$ is defined here. Thus we may put

$$\mathrm{Im}f(s^2)\rightarrow\frac{\pi}{6}\frac{(s^2-4\mu^2)^{\frac{3}{2}}}{s^5}|F_\pi(s^2)|^2. \tag{A6}$$

If we assume $|F_\pi(z)|^2$ is analytic in the upper half plane and does not go to infinity for $|z|\rightarrow\infty$, we may write the matrix element for the photon propagator with two-pion intermediate states (pion structure included) as

$$\frac{-1}{2}D_F'(q^2)g_{\mu\nu}=\frac{ig_{\mu\nu}}{(2\pi)^4}\frac{\alpha}{6\pi}\int_{4\mu^2}^{\infty}\frac{(s^2-4\mu^2)^{\frac{3}{2}}|F_\pi(s^2)|^2}{s^5(s^2-q^2-i\epsilon)}ds^2. \tag{A7}$$

Thus the matrix element for Fig. 9 can be written as

$$M_4(\text{pion pair})=-M_1\frac{\alpha}{6\pi}q^2\int_{4\mu^2}^{\infty}\frac{(s^2-4\mu^2)^{\frac{3}{2}}|F_\pi(s^2)|^2ds^2}{s^5(s^2-q^2-i\epsilon)}. \tag{A8}$$

Equation (A8) reduces to Eq. (A2) if pions are structureless, i.e., $|F_\pi(s^2)|^2=1$. We have made numerical integrations for Eq. (A8) with various forms of $|F_\pi(s^2)|^2$ given in reference 20. The results are still negligible,

namely less than 0.12% contribution to the cross section at 90° for Exp. I.

We have used the result obtained from the perturbation method in our derivation of Eq. (A7). However this is not necessary. We will show in the following that the same result can be obtained directly from the method of the spectral representation.[27] In terms of the spectral representation the matrix element for the photon propagator with two-pion intermediate states may be written as

$$-\tfrac{1}{2}D_F'(q^2)g_{\mu\nu}$$
$$=\frac{1}{(2\pi)^4}\int d^4x\, e^{iq\cdot x}\langle 0|\,T(A_\mu(x),A_\nu(0))\,|0\rangle$$
$$=\frac{-i}{(2\pi)^4}\int_{4\mu^2}^{\infty}\frac{\rho_{\mu\nu}(s^2)ds^2}{s^2-q^2-i\epsilon}, \tag{A9}$$

where

$$\rho_{\mu\nu}(s^2)=\tfrac{1}{3}g_{\mu\nu}\sum_n (2\pi)^3\delta^3(\mathbf{p}_n)2E_n\delta(p_n{}^2-s^2)$$
$$\times p_n{}^{-4}\langle 0|\,j_\lambda(0)\,|n\rangle\langle n|\,j^\lambda(0)\,|0\rangle, \tag{A10}$$

and p_n and E_n are four-momenta and energy of the intermediate state in the center-of-mass system. For an intermediate state consisting of mesons of four-momenta q_1 and q_2 with isotopic spin indices j and k, we may write[16,22]

$$\langle 0|\,j_\lambda(0)\,|n\rangle=\langle 0|\,j_\lambda(0)\,|q_1jq_2k\rangle$$
$$=\frac{ie}{(4\omega_1\omega_2)^{\frac{1}{2}}}(q_1-q_2)_\lambda(\delta_{j1}\delta_{k2}-\delta_{j2}\delta_{k1})F_\pi(p_n{}^2), \tag{A11}$$

where the factor $(\delta_{j1}\delta_{k2}-\delta_{j2}\delta_{k1})$ represents the system $\pi^+ + \pi^-$ which is odd under charge conjugation. Summing over the isotopic spin indices and contracting over λ, we have

$$\sum_{k,j=1}^{3}\langle 0|\,j_\lambda(0)\,|q_1jq_2k\rangle\langle q_1jq_2k|\,j^\lambda(0)\,|0\rangle$$
$$=\frac{-2e^2(p_n{}^2-4\mu^2)}{4\omega_1\omega_2}|F_\pi(p_n{}^2)|^2. \tag{A12}$$

Hence, from Eqs. (A10) and (A12), we have

$$\rho_{\mu\nu}(s^2)$$
$$=\frac{-q_{\mu\nu}}{3}\frac{2e^2}{(2\pi)^3}\int\frac{d^3q_1}{2\omega_1}\int\frac{d^3q_2}{2\omega_2}\delta^3(\mathbf{q}_1+\mathbf{q}_2)2(\omega_1+\omega_2)$$
$$\times\delta(p_n{}^2-s^2)\frac{|F_\pi(p_n{}^2)|^2}{p_n{}^4}(p_n{}^2-4\mu^2)$$
$$=-g_{\mu\nu}\frac{\alpha}{6\pi}\frac{(s^2-4\mu^2)^{\frac{3}{2}}|F_\pi(s^2)|^2}{s^5}. \tag{A13}$$

Substituting Eq. (A13) into Eq. (A9), we obtain exactly Eq. (A7). Thus, we have obtained the same result as before without the help of the perturbation method.

It is instructive to notice that the matrix element for the photon propagator with two-pion intermediate states [Eq. (A7)] can be expressed (other than a constant factor) as a Hilbert transform of the total cross section of the process $e^+ + e^- \to \pi^+ + \pi^-$ in the center-of-mass system [integrate Eq. (58) over the solid angles and let $F_\lambda{}^2(s^2)c^2(s^2)=1$].

[27] G. Källén, Helv. Phys. Acta **25**, 417 (1952).